CARBON and OXYGEN

SHELL-NODAL STRUCTURE

George P. Shpenkov

http://shpenkov.janmax.com/CarbonOxygen.pdf

Particular solutions of the wave equation in spherical polar coordinates

$$\Delta\hat{\Psi} - \frac{1}{c^2}\frac{\partial^2\hat{\Psi}}{\partial t^2} = 0 \qquad (1)$$

The wave equation (1) admits the particular solutions in the form

$$\hat{\Psi}(\mathbf{r},t) = \hat{\psi}(\mathbf{r})e^{\pm i\omega t} \quad (\omega = kc) \qquad (2)$$

where

$$\hat{\psi}(\mathbf{r}) = \hat{R}(kr)\Theta(\theta)\hat{\Phi}(\varphi)$$

is a particular solution of the corresponding Helmholtz equation

$$\Delta\hat{\psi} + k^2\hat{\psi} = 0\,; \qquad (3)$$

The separation of variables leads to one time equation

$$\frac{d^2\hat{T}}{d\tau^2} = -\hat{T} \qquad (4)$$

and ***three equations of the spherical space***:

$$\rho^2 \frac{d^2 \hat{R}_l}{d\rho^2} + 2\rho \frac{d\hat{R}_l}{d\rho} + (\rho^2 - l(l+1))\hat{R}_l = 0 \tag{5}$$

$$\frac{d^2 \Theta_{l,m}}{d\theta^2} + ctg\theta \frac{d\Theta_{l,m}}{d\theta} + \left(l(l+1) - \frac{m^2}{\sin^2 \theta} \right) \Theta_{l,m} = 0 \tag{6}$$

$$\frac{d^2 \hat{\Phi}_m}{d\varphi^2} + m^2 \hat{\Phi}_m = 0 \tag{7}$$

where $\rho = kr$ and $\tau = \omega t$.

The ***time component*** is usually presented in the form

$$\hat{T}(\omega t) = e^{i\omega t} \tag{8}$$

The ***general form of the solutions*** of the wave equation (1) for the spherical (longitudinal, central) component of $\hat{\Psi}$, ***in spherical polar coordinates***, is

$$\hat{\Psi} = \hat{R}_l(kr)\Theta_{l,m}(\theta)\hat{\Phi}_m(\varphi)\hat{T}(\omega t) \tag{9}$$

where $\hat{\psi} = \hat{R}_l(kr)\Theta_{l,m}(\theta)\hat{\Phi}_m(\varphi)$ is the ***spatial factor*** of the wave function of physical space; $l = 0,1,2,\ldots$; $m = 0,\pm 1,\pm 2,\ldots,\pm l$.

The ***radial component*** $\hat{R}_l(kr)$ of the spatial factor describes the ***density of potential-kinetic probability of radial displacements***, the ***polar component*** $\Theta_{l,m}(\theta)$ – the ***polar displacements***, and $\hat{\Phi}_m(\varphi)$ – the ***azimuth displacements***.

Under the above conditions, at integer values of the wave number *m*, an ***elementary solution of the wave equation has the standard form***. If we present the number *m* in the form $m = \frac{1}{2}2s$, where $s \in N$, we arrive at

$$\hat{\psi} = A_l \hat{R}_l(\rho)\Theta_{l,s}(\theta)e^{\pm is\varphi} = A_l\sqrt{\pi/2\rho}H^{\pm}_{l+1/2}(\rho)\Theta_{l,s}(\theta)e^{\pm is\varphi} \qquad (10)$$

or

$$\hat{\psi} = A_l\sqrt{\pi/2\rho}(J_{l+1/2}(\rho) \pm iY_{l+1/2}(\rho))\Theta_{l,s}(\theta)e^{\pm is\varphi}, \qquad (11)$$

where A_l is the constant factor; $\rho = kr$;

$H^{\pm}_{l+1/2}(\rho)$, $J_{l+1/2}(\rho)$ and $Y_{l+1/2}(\rho)$ (or $N_{l+1/2}(\rho)$) are the Hankel, Bessel and Neumann functions, correspondingly.

Two terms in (11) are the ***potential*** and ***kinetic spatial constituents*** of $\hat{\Psi}$ function; they have the following form

$$\hat{\psi}_p = Ac_l(\rho)/\rho = A\sqrt{\pi/2\rho}J_{l+1/2}(\rho)\Theta_{l,m}(\theta)e^{\pm im\varphi} \tag{12}$$

$$\hat{\psi}_k = \pm As_l(\rho)/\rho = \pm A\sqrt{\pi/2\rho}Y_{l+1/2}(\rho)\Theta_{l,m}(\theta)e^{\pm im\varphi} \tag{13}$$

The ***half-integer solutions*** of (3), at $l = m = (1/2)s$, have the form

$$\hat{\psi} = A\hat{R}_s(\rho)\Theta_s(\theta)e^{\pm i\frac{s}{2}\varphi} \tag{14}$$

where

$$\hat{R}_s(\rho) = \sqrt{\pi/2\rho}H^{\pm}_{\frac{s}{2}+\frac{1}{2}}(\rho) \tag{15}$$

$$\Theta_s(\theta)e^{\pm i\frac{s}{2}\varphi} = C_s \sin^{\frac{s}{2}}\theta(\cos\frac{s}{2}\varphi \pm i\sin\frac{s}{2}\varphi) \tag{16}$$

The polar extremes of half-integer solutions lie in the equatorial plane.

The Radial Solutions for the Wave Equation

l	$\hat{R}_l(\rho)/A = \hat{e}_l(\rho)/\rho = \sqrt{\pi/2\rho}\,(J_{l+1/2}(\rho) \pm iY_{l+1/2}(\rho))$
0	$(\sin\rho \pm i\,(-\cos\rho))/\rho$
1	$((\rho^{-1}\sin\rho - \cos\rho) \pm i\,(-\rho^{-1}\cos\rho - \sin\rho))\,\rho^{-1}$
2	$[((3\rho^{-2} - 1)\sin\rho - 3\rho^{-1}\cos\rho)) \pm i\,((1 - 3\rho^{-2})\cos\rho - 3\rho^{-1}\sin\rho))]\,\rho^{-1}$
3	$[((15\rho^{-3} - 6\rho^{-1})\sin\rho + (1 - 15\rho^{-2})\cos\rho) \pm i(-(15\rho^{-3} - 6\rho^{-1})\cos\rho + +(1 - 15\rho^{-2})\sin\rho)]\rho^{--1}$
4	$[((1 - 45\rho^{-2} + 105\rho^{-4})\sin\rho + (10\rho^{-1} - 105\rho^{-3})\cos\rho) \pm \pm i\,(-(1 - 45\rho^{-2} + 105\rho^{-4})\cos\rho + (10\rho^{-1} - 105\rho^{-3})\sin\rho)]\,\rho^{-1}$
5	$[((945\rho^{-5} - 420\rho^{-3} + 15\rho^{-1})\sin\rho - (945\rho^{-4} - 105\rho^{-2} + 1)\cos\rho) \pm \pm i\,(-(945\rho^{-5} - 420\rho^{-3} + 15\rho^{-1})\cos\rho - (945\rho^{-4} - 105\rho^{-2} + 1)\sin\rho)]\,\rho^{-1}$

Plots of the First Six Radial Spherical Functions

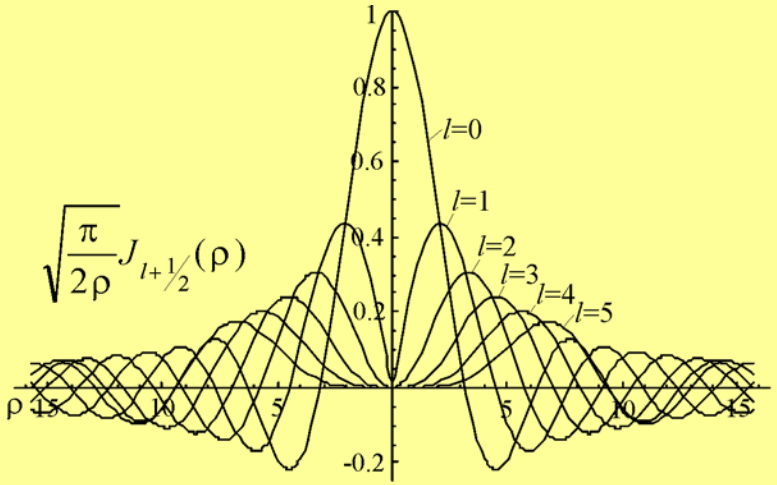

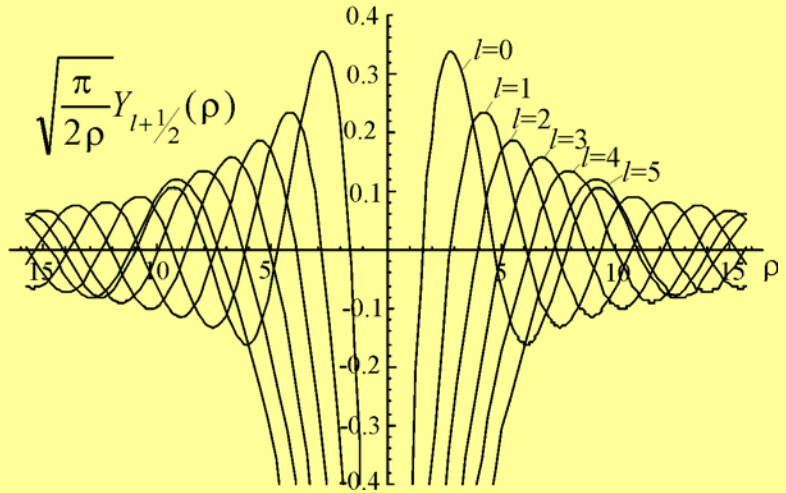

Reduced Polar-Azimuthal Potential Functions

l	m	$\tilde{V}_{l,m}(\theta,\varphi) = \tilde{\theta}_{l,m}(\theta)\cos m\varphi$	l	m	$\tilde{V}_{l,m}(\theta,\varphi) = \tilde{\theta}_{l,m}(\theta)\cos m\varphi$
0	0	1			
1	0	$\cos\theta$	5	0	$\cos\theta\,(\cos^4\theta - 10/9\cos^2\theta + 5/21)$
	±1	$\sin\theta\cos\varphi$		±1	$\sin\theta\,(\cos^4\theta - 2/3\cos^2\theta + 1/21)\cos\varphi$
2	0	$\cos^2\theta - 1/3$		±2	$\sin^2\theta\cos\theta\,(\cos^2\theta - 1/3)\cos 2\varphi$
	±1	$\sin\theta\cos\theta\cos\varphi$		±3	$\sin^3\theta\,(\cos^2\theta - 1/9)\cos 3\varphi$
	±2	$\sin^2\theta\cos 2\varphi$		±4	$\sin^4\theta\cos\theta\cos 4\varphi$
3	0	$\cos\theta\,(\cos^2\theta - 3/5)$		±5	$\sin^5\theta\cos 5\varphi$
	±1	$\sin\theta\,(\cos^2\theta - 1/5)\cos\varphi$			
	±2	$\sin^2\theta\cos\theta\cos 2\varphi$	6	0	$\cos^6\theta - 15/11\cos^4\theta + 5/11\cos^2\theta - 5/231$
	±3	$\sin^3\theta\cos 3\varphi$		±1	$\sin\theta\cos\theta\,(\cos^4\theta - 10/11\cos^2\theta + 5/33)\cos\varphi$
4	0	$\cos^4\theta - 6/7\cos^2\theta + 3/35$		±2	$\sin^2\theta\,(\cos^4\theta - 6/11\cos^2\theta + 1/33)\cos 2\varphi$
	±1	$\sin\theta\cos\theta\,(\cos^2\theta - 3/7)\cos\varphi$		±3	$\sin^3\theta\cos\theta\,(\cos^2\theta - 3/11)\cos 3\varphi$
	±2	$\sin^2\theta\,(\cos^2\theta - 1/7)\cos 2\varphi$		±4	$\sin^4\theta\,(\cos^2\theta - 1/11)\cos 4\varphi$
	±3	$\sin^3\theta\cos\theta\cos 3\varphi$		±5	$\sin^5\theta\cos\theta\cos 5\varphi$
	±4	$\sin^4\theta\cos 4\varphi$		±6	$\sin^6\theta\cos 6\varphi$

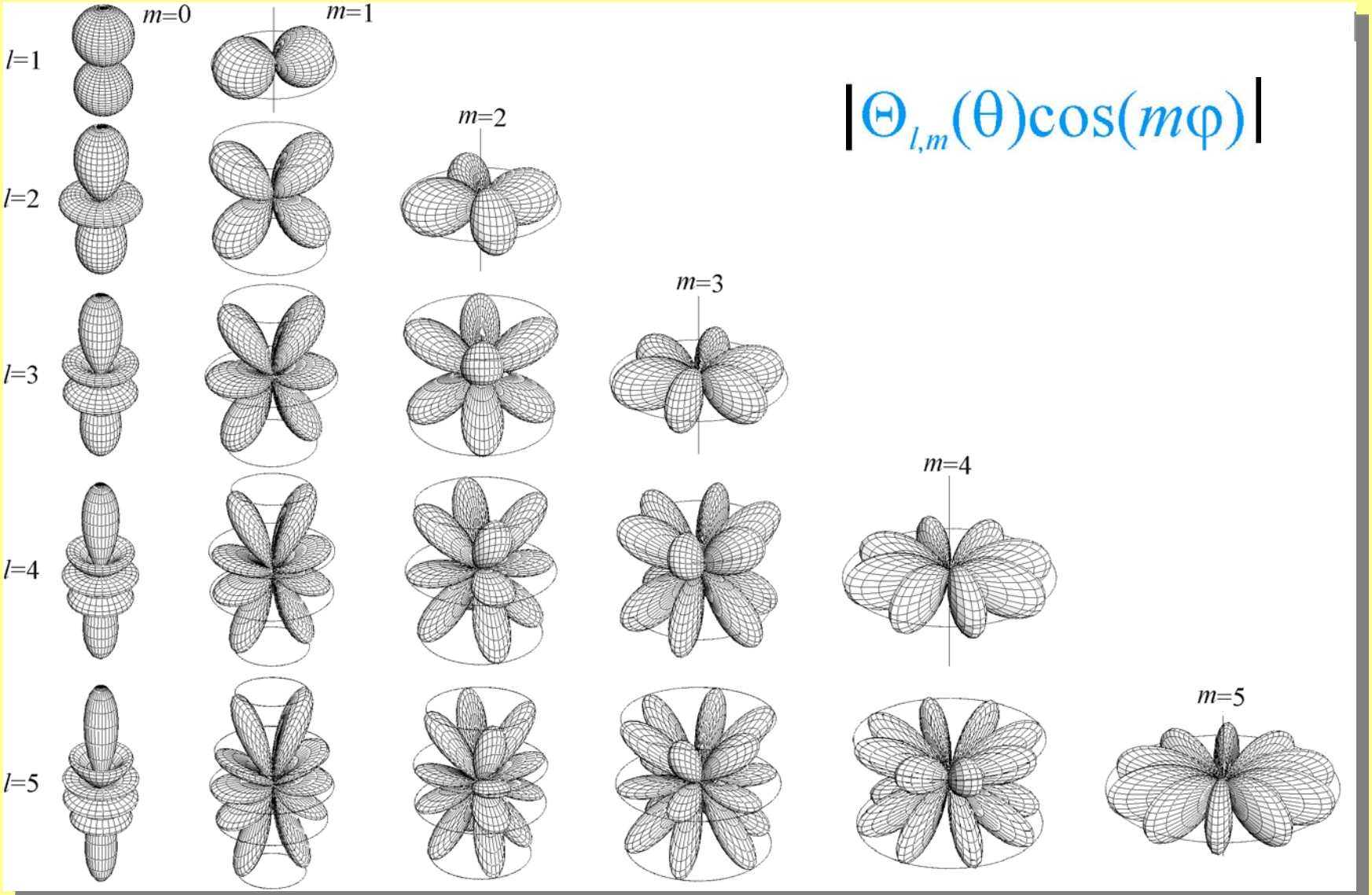

Graphs of the polar-azimuthal functions

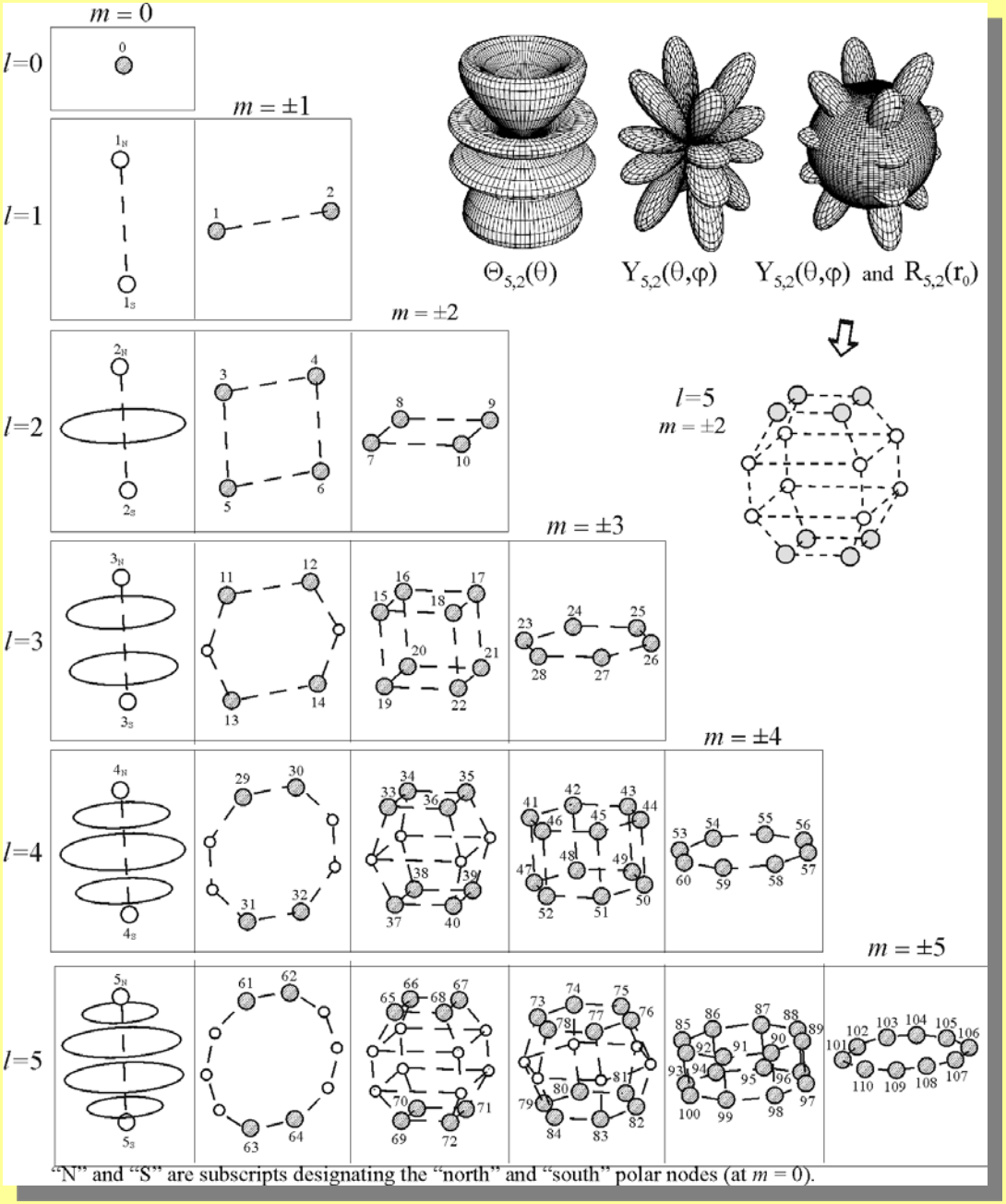

A spatial disposition of polar nodes and rings (m=0), and polar-azimuthal potential nodes (m≠0)

(soltutions of the wave equation)

$$\Delta\hat{\Psi} - \frac{1}{c^2}\frac{\partial^2\hat{\Psi}}{\partial t^2} = 0$$

A schematic drawing of the nodes and a toroidal vortex-ring in the carbon and neon atoms

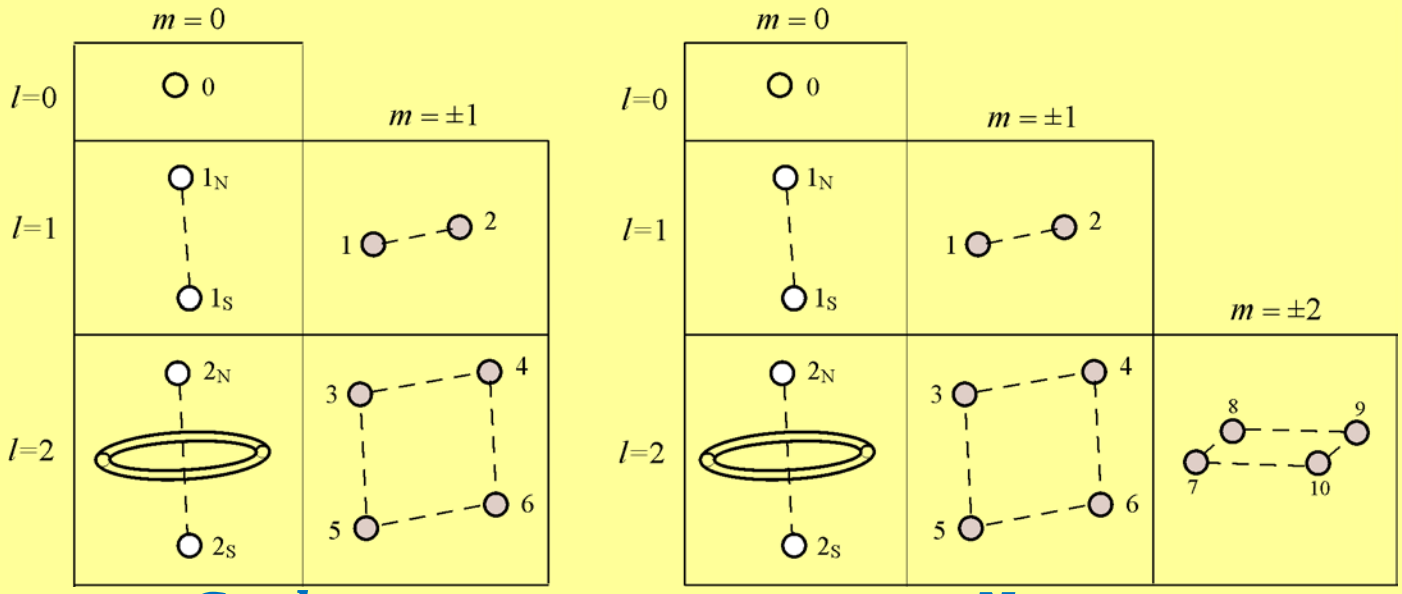

Carbon Neon

0, 1_N, 1_S, 2_N, 2_S are the ordinal number of the polar potential-kinetic nodes (located along the z-axis, m = 0); 1, 2,..., 10 are the ordinal numbers of principal polar-azimuthal potential nodes. The nodes 1 and 2 belong to the internal spherical shell, l = 1; the nodes 3 - 10 are located on the external spherical shell, l = 2.

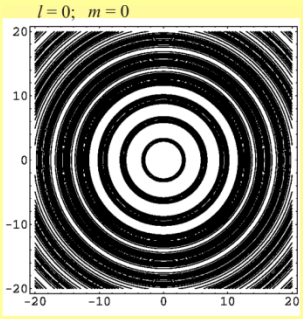

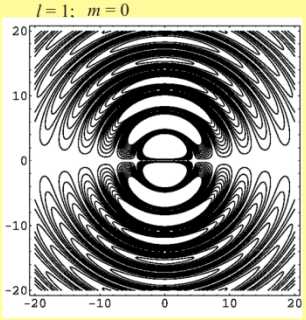

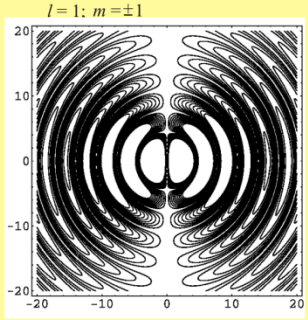

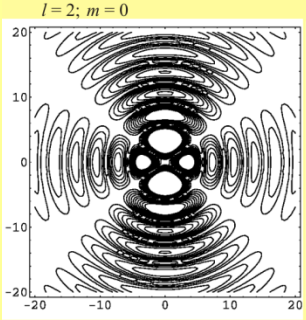

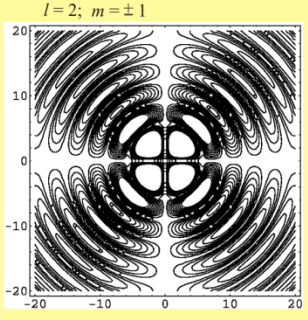

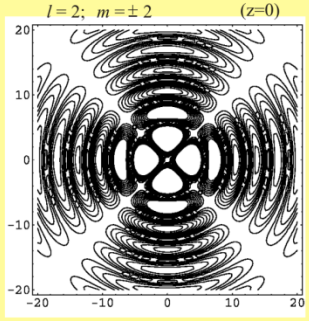

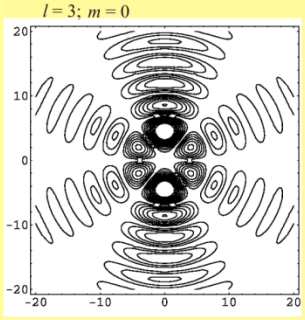

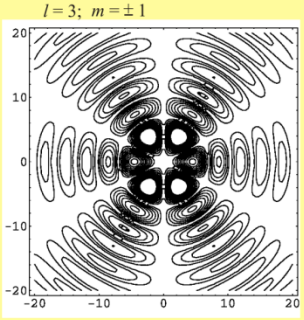

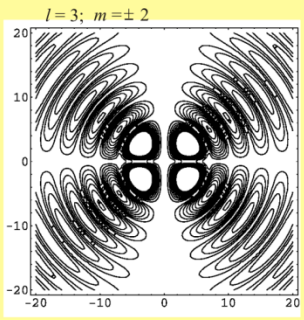

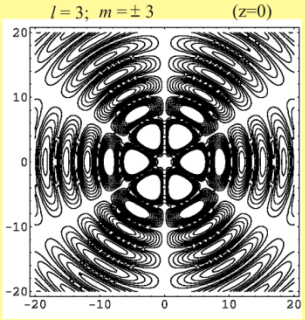

Contour plots of sections for the potential density of probability Ψ_p in a plane x=0 (and z=0 for l=2, m=± 2; l=3, m=±3)

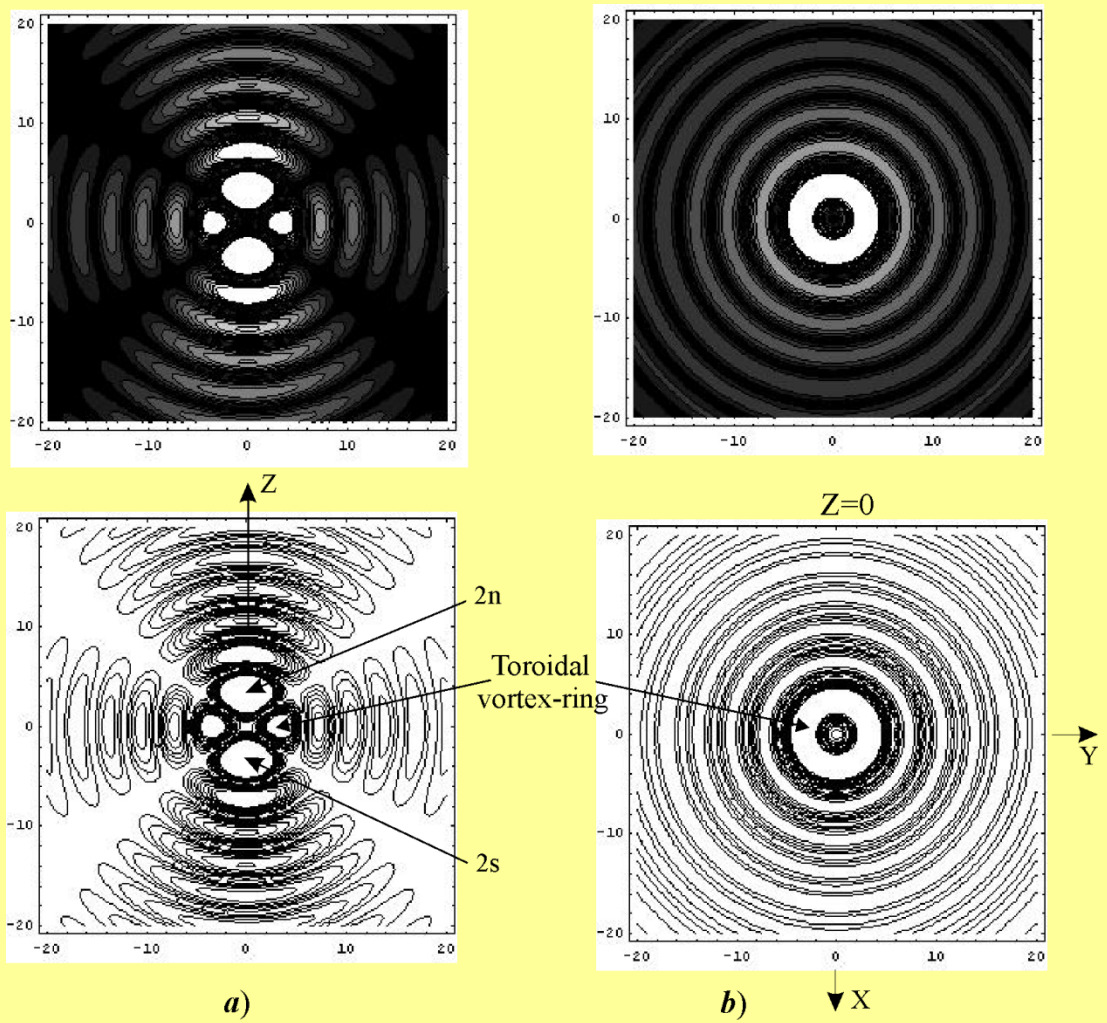

A solution of the wave equation for a spherical shell of the atoms with the wave (quantum) numbers $l = 2$, $m = 0$: (*a*) for a section along the *z*-axis (in a plane perpendicular to the plane (*x*, *y*)), (*b*) for a section $z = 0$ in a plane (*x*, *y*); 2*n* and 2*s* are, respectively, the north and south polar nodes of the shell

PERIODIC TABLE

OF THE ELEMENTS

$$\Delta\hat{\Psi}-\frac{1}{c^2}\frac{\partial^2\hat{\Psi}}{\partial t^2}=0$$

The simplest solutions of the wave probabilistic equation presented in the form of spatial distribution of *potential* nodes (discrete elements of the ***shell-nodal structure*** of atoms) and in a traditional form of a periodic table [1-3]: $\Psi_{l,m}(\rho,\theta,\varphi)_p=C_\Psi R_l(\rho)\Theta_{l,m}(\theta)\mathrm{Cos}m\varphi$, where C_Ψ is the constant factor, $\rho = kr$ is the relative radius of the characteristic shells, θ and φ are polar and azimuth angles, respectively.

Numbers 1, 2, 3, … , 110 are the ordinal numbers of the ***principal polar-azimuth nodes*** coinciding with the atomic numbers of elements *Z*.

The unnumbered ***collateral polar-azimuth nodes***

Elements with the completely filled outer nucleonic shells

$_2$He				
$_6$C	$_{10}$Ne			
$_{14}$Si	$_{22}$Ti	$_{28}$Ni		
$_{32}$Ge	$_{40}$Zr	$_{52}$Te	$_{60}$Nd	
$_{64}$Gd	$_{72}$Hf	$_{84}$Po	$_{100}$Fm	$_{110}$Ds

is the designation of unstable elements

Polar nodes and rings

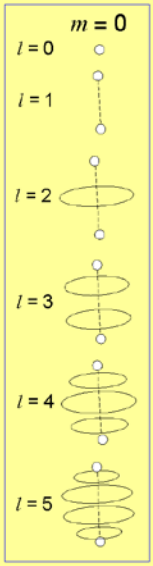

[1] *Alternative Picture of the World*, V. 1-3, (1996); [2] *Foundations of Physics*, (1998); [3] *Atomic Structure of Matter-Space*, (2001); Geo. S., Bydgoszcz by L. Kreidik and G. Shpenkov.
The Shell Structure of Matter Spaces, **http://shpenkov.janmax.com/ShellStr.pdf**

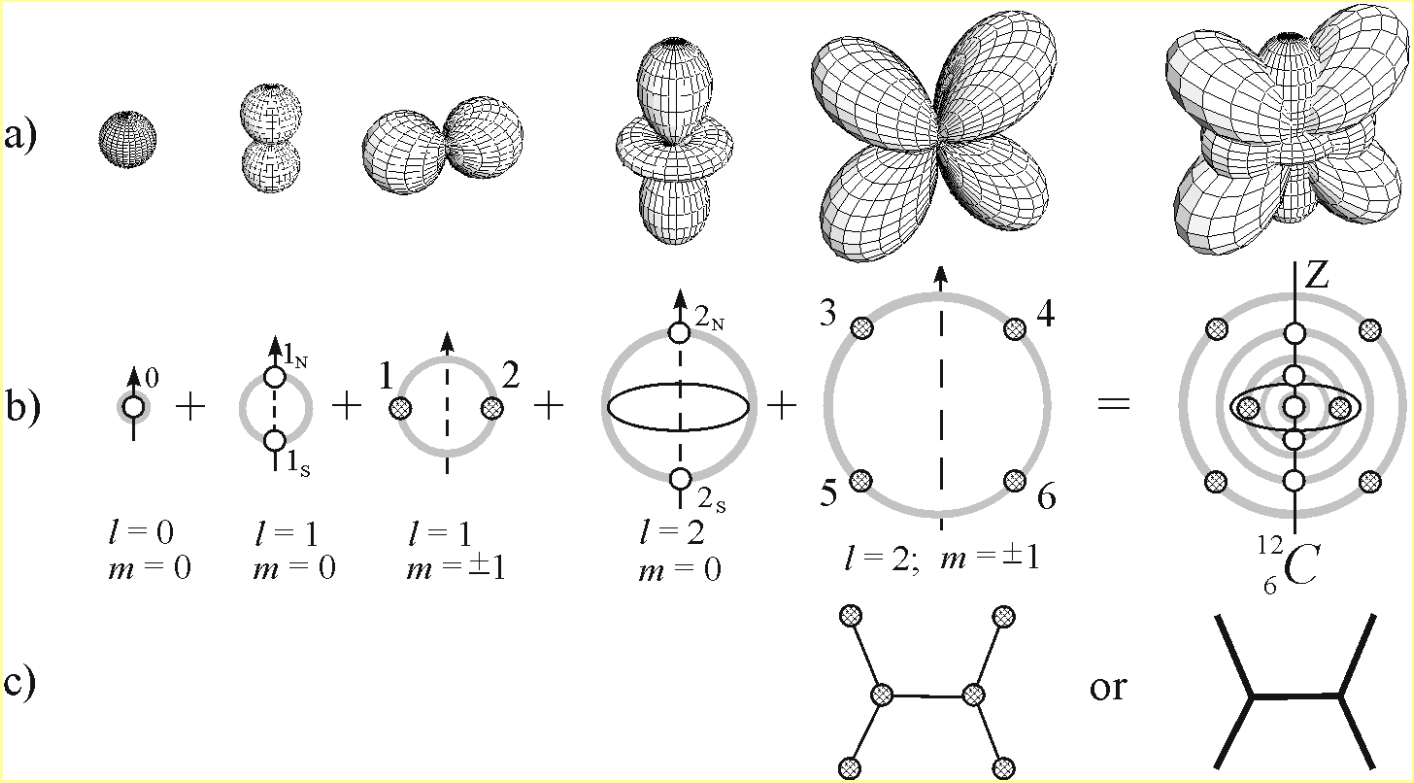

(a) Plots of potential-kinetic polar and potential polar-azimuthal functions;
(b) polar and potential nodes on spherical shells;
(c) symbolic designations of the carbon atom

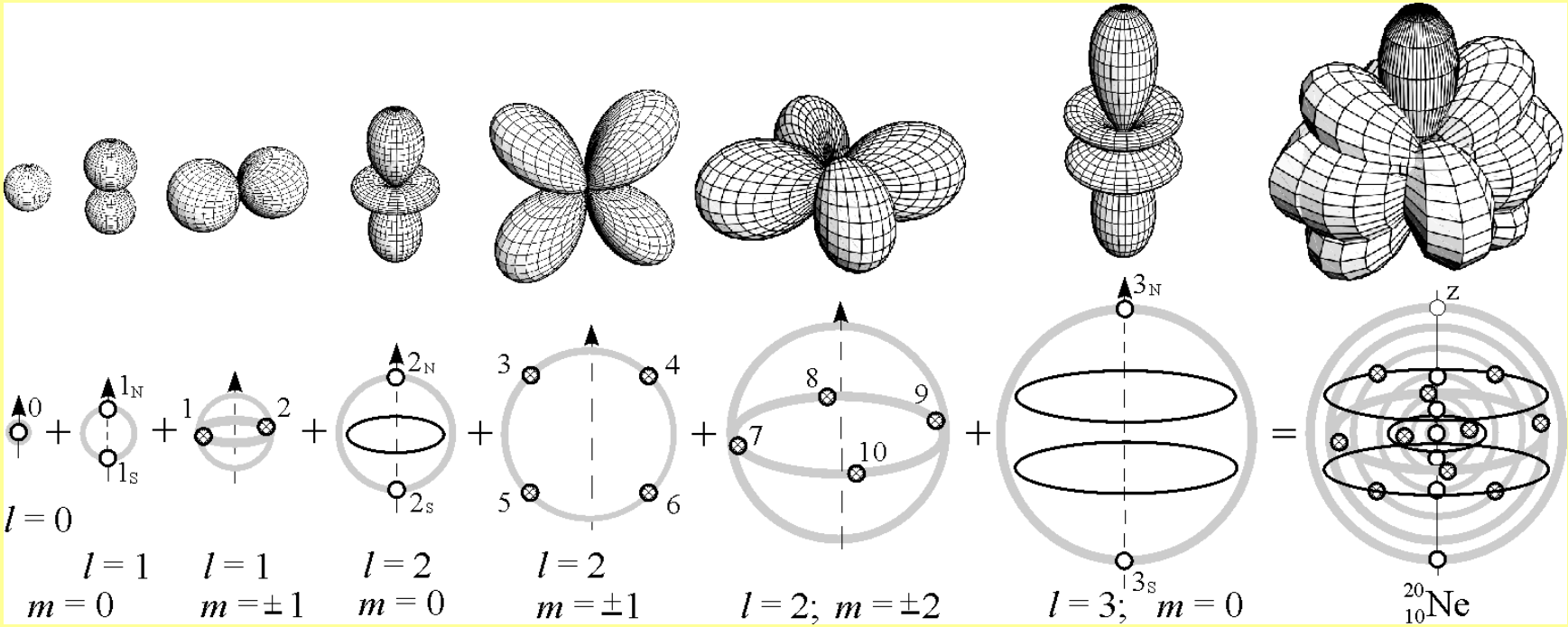

(a) Plots of potential-kinetic polar and potential polar-azimuthal functions;
(b) polar and potential nodes on spherical shells;
(c) symbolic designations of the neon atom

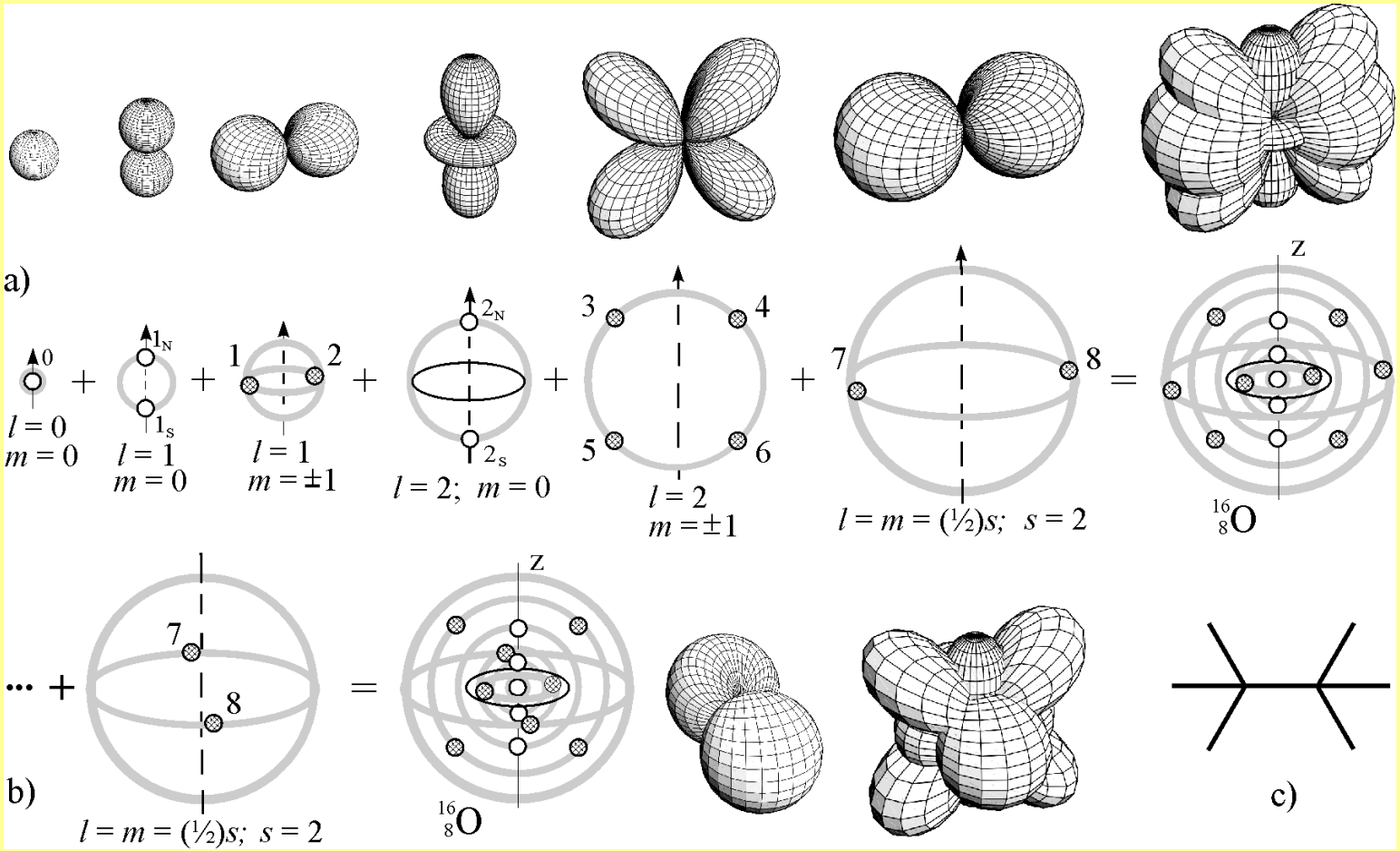

(a) Plots of potential-kinetic polar and potential polar-azimuthal functions;
(b) polar and potential nodes on spherical shells;
(c) symbolic designations of the oxygen atom

The Relative Atomic Mass

$$A = \sum_{k} Z_{pk}\eta_{pk} + \sum_{i} (Z_{gi}\eta_{gi} + Z_{vi}\eta_{vi})$$

k, i are the numbers of polar ($m = 0$) and polar-azimuthal ($m \neq 0$) shells, respectively;

$Z_{p,k}$ is the number of polar nodes of *k*-th polar shell;

Z_{gi} and Z_{vi} are the number of principal and collateral polar-azimuth nodes, respectively, of *i*-th polar-azimuthal shell;

η_{pk}, η_{gi}, and η_{vi} = 0, 1, or 2 is the multiplicity of filling of the nodes by H-atoms.

The Matrices of the Nodes of Carbon and Oxygen Atoms

(potential-kinetic polar and potential polar-azimuthal)

$$|C_{l,m}| = \begin{vmatrix} 1 & 0 & 0 \\ 2 & 2 & 0 \\ 2 & 4 & 0 \end{vmatrix} \qquad |O_{l,m}| = \begin{vmatrix} 1 & 0 & 0 \\ 2 & 2 & 0 \\ 2 & 4 & 2 \end{vmatrix}$$

The matrices of filing of the nodes by H-atoms in the stable, lightest, and heaviest isotopes of the carbon and oxygen atoms

$$|{}^{12}_{6}C| = \begin{vmatrix} 0 & 0 & 0 \\ 0 & 4 & 0 \\ 0 & 8 & 0 \end{vmatrix} \qquad |{}^{8}_{6}C| = \begin{vmatrix} 0 & 0 & 0 \\ 0 & 4 & 0 \\ 0 & 4 & 0 \end{vmatrix} \qquad |{}^{22}_{6}C| = \begin{vmatrix} 2 & 0 & 0 \\ 4 & 4 & 0 \\ 4 & 8 & 0 \end{vmatrix}$$

$$|{}^{16}_{8}O| = \begin{vmatrix} 0 & 0 & 0 \\ 0 & 4 & 0 \\ 0 & 8 & 4 \end{vmatrix} \qquad |{}^{12}_{8}O| = \begin{vmatrix} 0 & 0 & 0 \\ 0 & 4 & 0 \\ 0 & 6 & 2 \end{vmatrix} \qquad |{}^{12}_{8}O| = \begin{vmatrix} 0 & 0 & 0 \\ 0 & 4 & 0 \\ 0 & 4 & 4 \end{vmatrix} \qquad |{}^{26}_{6}C| = \begin{vmatrix} 2 & 0 & 0 \\ 4 & 4 & 0 \\ 4 & 8 & 4 \end{vmatrix}$$

Isotopes of Carbon

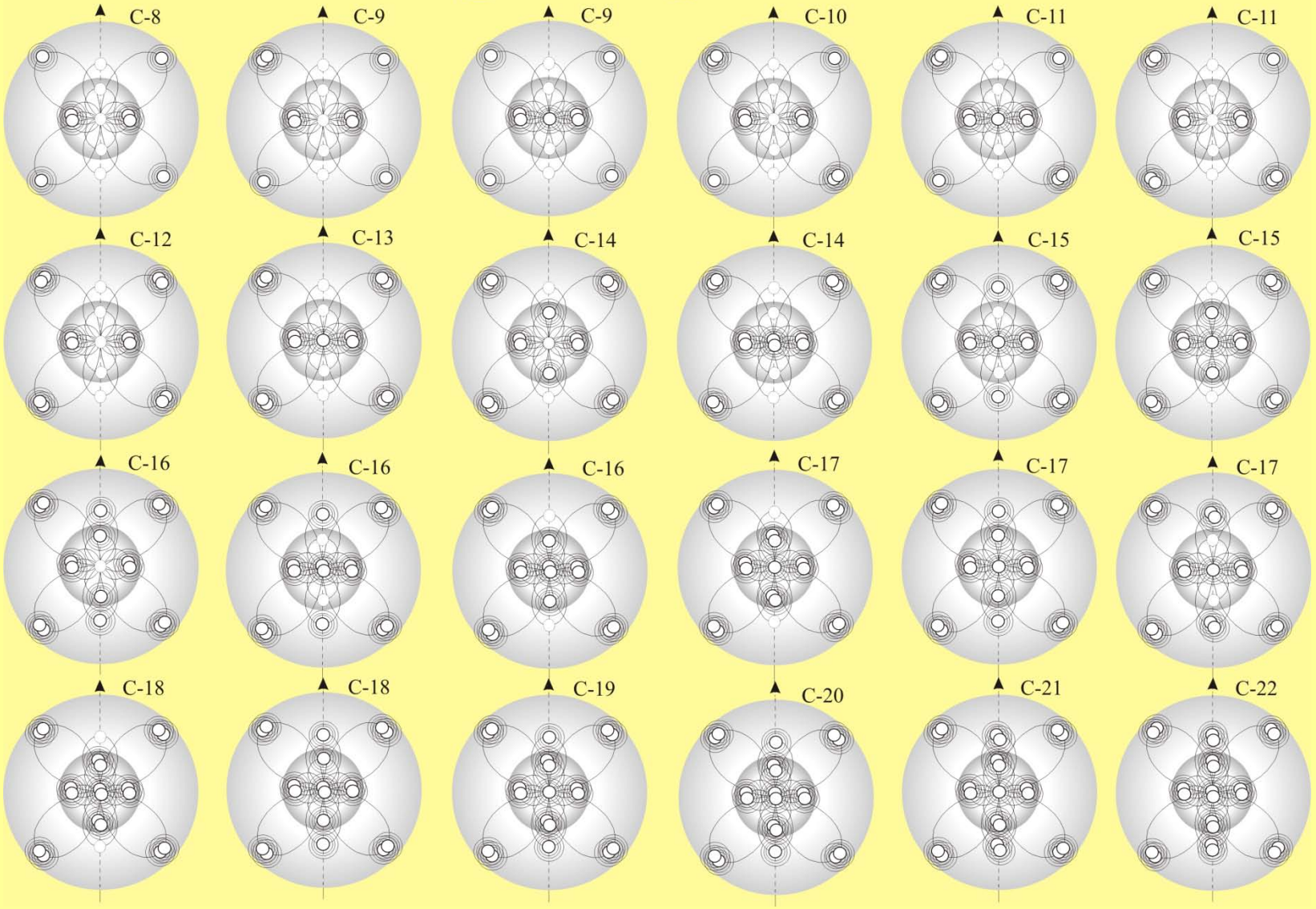

The shell-nodal structure of some isotopes of oxygen:

3 stable (^{16}O, ^{17}O and ^{18}O) and 5 short-lived unstable (including lightest ^{12}O and heaviest ^{26}O)

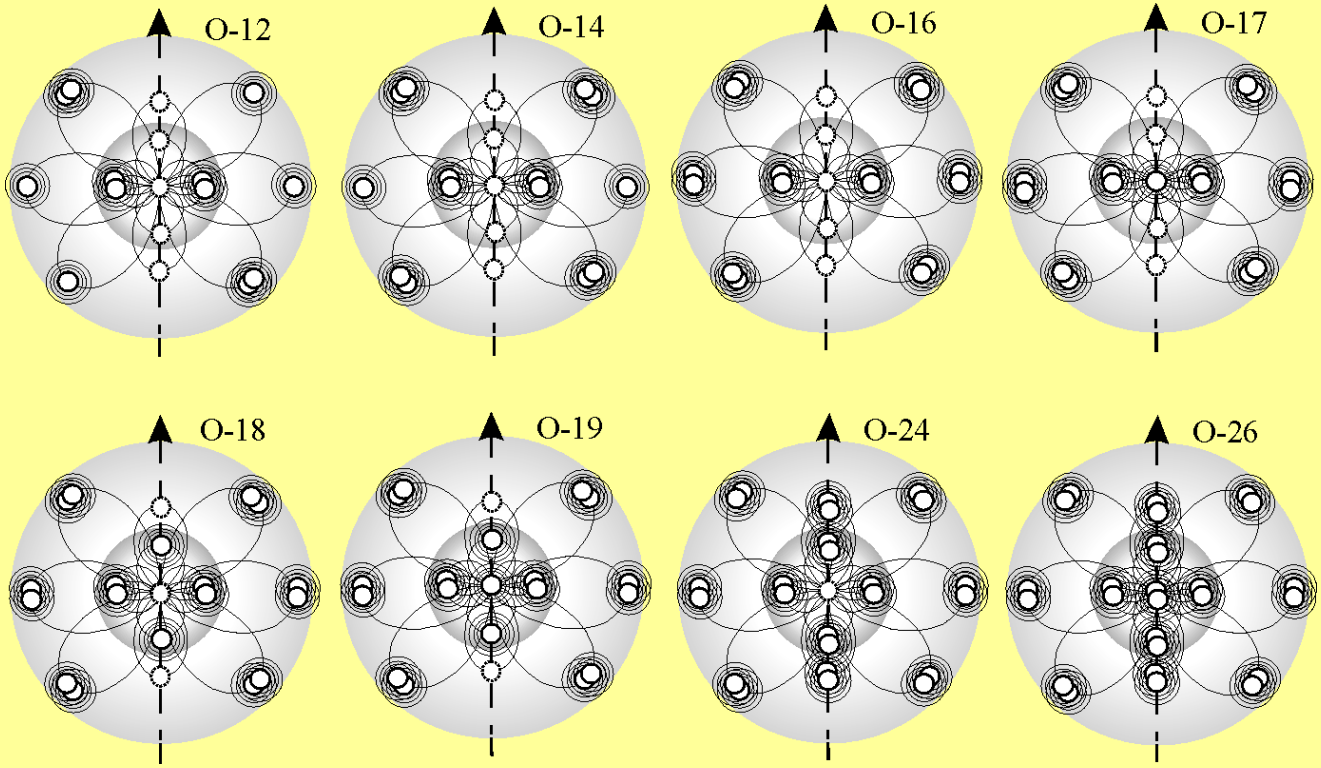

RELATIVE ATOMIC MASSES OF THE ELEMENTS

The particular solutions of the wave probabilistic equation $\Delta\hat{\Psi} - \frac{1}{c^2}\frac{\partial^2\hat{\Psi}}{\partial t^2} = 0$ [1-3]

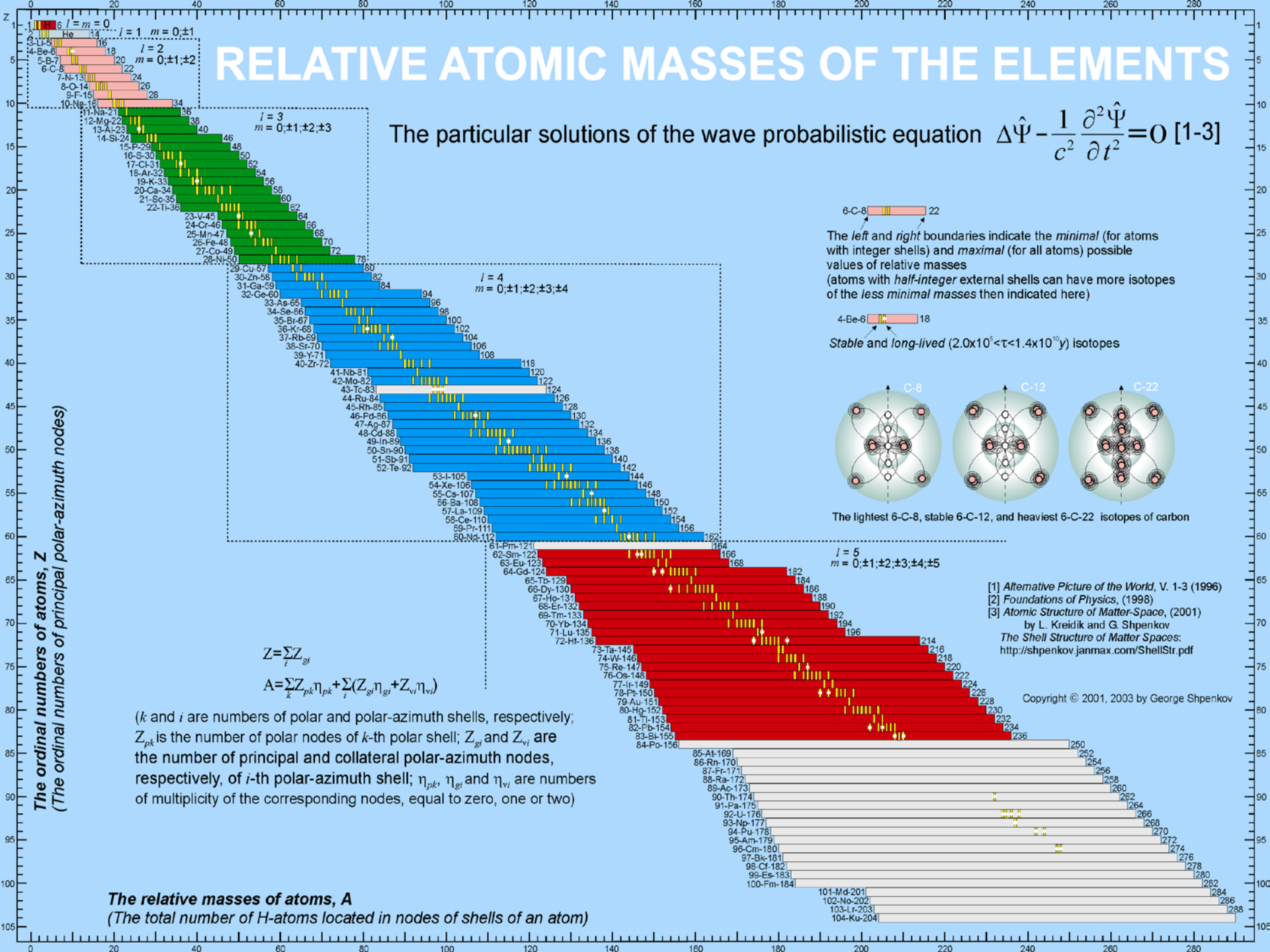

6-C-8 22

The *left* and *right* boundaries indicate the *minimal* (for atoms with integer shells) and *maximal* (for all atoms) possible values of relative masses
(atoms with *half-integer* external shells can have more isotopes of the *less minimal masses* then indicated here)

4-Be-6 18

Stable and *long-lived* ($2.0\times10^{5}<\tau<1.4\times10^{10}$ *y*) isotopes

The lightest 6-C-8, stable 6-C-12, and heaviest 6-C-22 isotopes of carbon

The ordinal numbers of atoms, Z
(The ordinal numbers of principal polar-azimuth nodes)

$$Z=\sum_i Z_{gi}$$

$$A=\sum_k Z_{pk}\eta_{pk}+\sum_i (Z_{gi}\eta_{gi}+Z_{vi}\eta_{vi})$$

(k and i are numbers of polar and polar-azimuth shells, respectively; Z_{pk} is the number of polar nodes of k-th polar shell; Z_{gi} and Z_{vi} are the number of principal and collateral polar-azimuth nodes, respectively, of i-th polar-azimuth shell; η_{pk}, η_{gi} and η_{vi} are numbers of multiplicity of the corresponding nodes, equal to zero, one or two)

The relative masses of atoms, A
(The total number of H-atoms located in nodes of shells of an atom)

[1] *Alternative Picture of the World*, V. 1-3 (1996)
[2] *Foundations of Physics*, (1998)
[3] *Atomic Structure of Matter-Space*, (2001)
by L. Kreidik and G. Shpenkov
The Shell Structure of Matter Spaces:
http://shpenkov.janmax.com/ShellStr.pdf

The Carbon Atom Structure

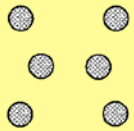

Direct image of the atom

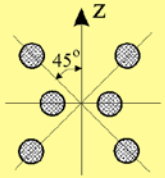

Position of the Z axis

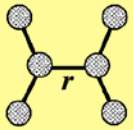

Main internodal bonds

(is an image of the potential node filled with 2 nucleons)

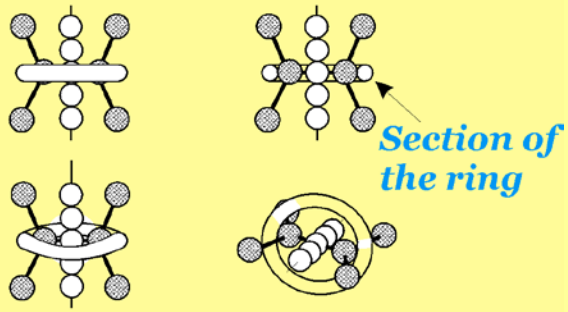

*Position of **polar nodes** and a **toroidal ring***

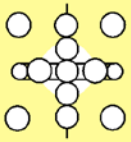

*Position of polar and **kinetic nodes** and a toroidal ring*

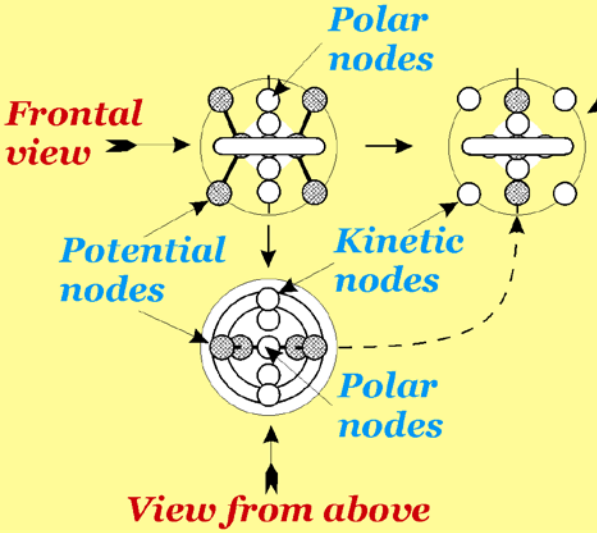

Mutual position of all constituents of the atom in three projections with indication of main bonds and external spherical shell

Conditional designation of the atom

An elementary cell of graphite

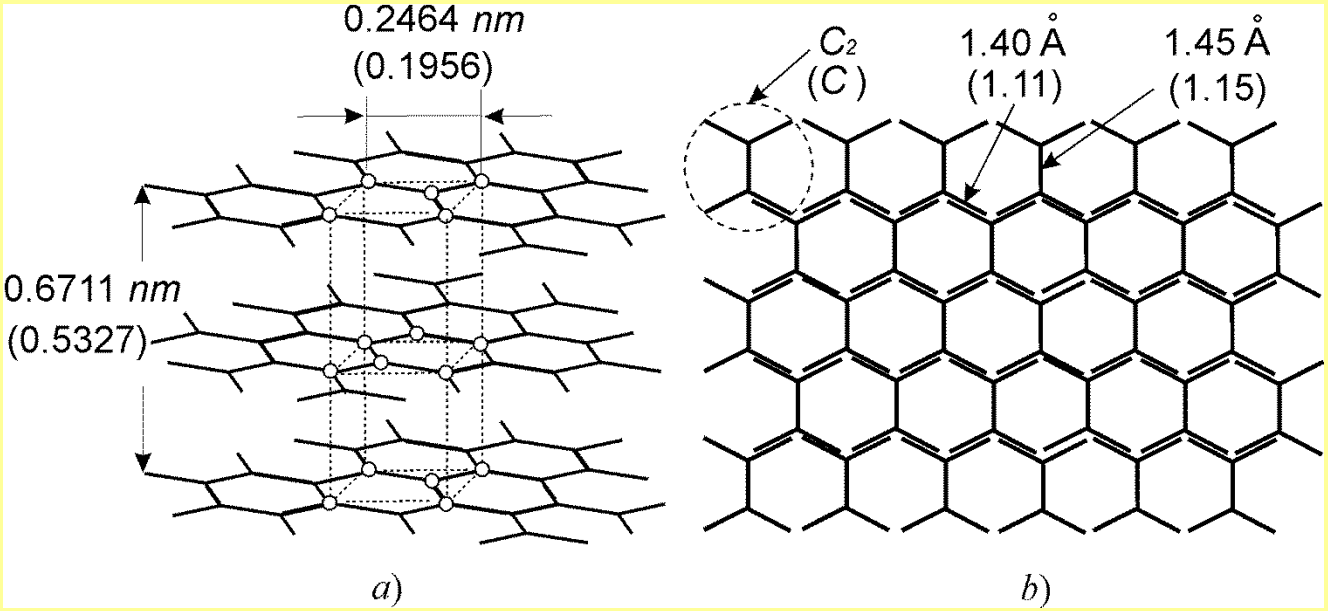

Lattice constants of graphite indicated in brackets correspond to Imaginary crystal lattice parameters if one account that the lattice is formed from single carbon atoms.

Formation of the C2 Molecule

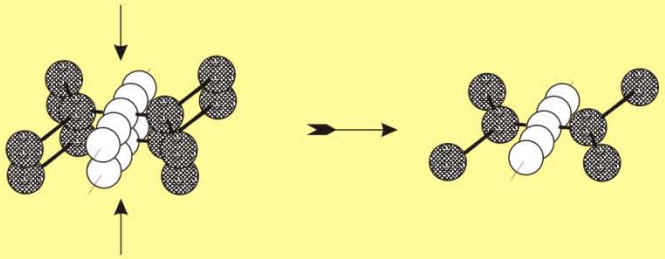

$C + C \longrightarrow C_2$

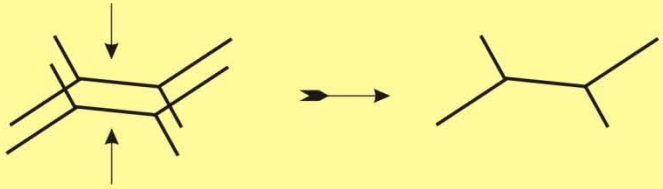

Overlapping, "confluence", of all approaching nodes (and toroidal rings not shown here) of two carbon atoms in the unit whole.

(An image of C2 does not differ from the image of a single C atom)

Precise calculations of atomic positions and the length of interatomic bonds are based on an iterative method. The latter includes a comparison and fitting of measured intensities of a reflected beam with calculated ones and with due account of Rutherford-Bohr's nuclear model of atoms, so as long as will not be achieved an adequate correspondence of two sets of the values.

Obviously, if only a structural analysis would be based on a shell-nodal (i.e., multi-center or molecule-like) atomic model, the gauging would be different; depending on what is accepted in the capacity of an elementary "building block" of crystal lattices – a molecule-like atom or a carbon dimer, C or C_2 in our case.

Assuming that the lattice constants of crystals accepted in physics are precise and congruent to reality, we must accept that an elementary "building block" of carbon crystals is the C_2 diatomic molecule.

Carbon Dimer (C2)

is

in fact the major observable product of C_{60} fragmentation.

Being a very effective growth species, it can rapidly incorporate into the diamond lattice leading to high-film growth rates*.

*** [D. M. Gruen, at al, *Turning Soot Into Diamonds With Microwaves*, Proceedings of the 29th Microwave Power Symposium, Chicago, Illinois, July 25-27, 1994].**

And as follows from the work referred below,

"the C_2 radical was considered to be responsible for the formation of graphite"**

**** [H. C. Shik, et al., *Diamond and Related Materials*, 2, 531 (1993)],**

A schematic view of self-binding (assembling) of two-dimensional carbon compounds

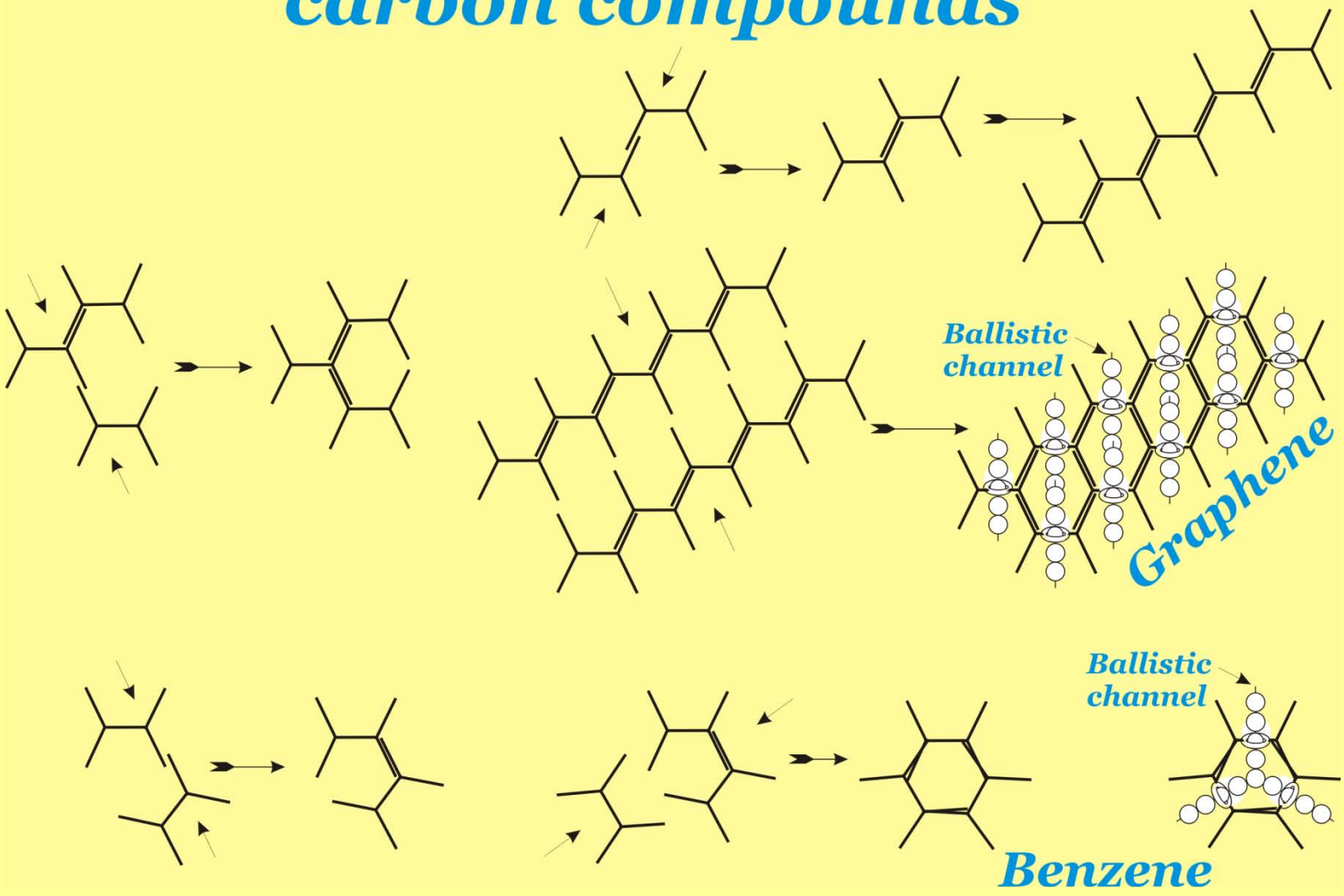

A part of a graphene sheet

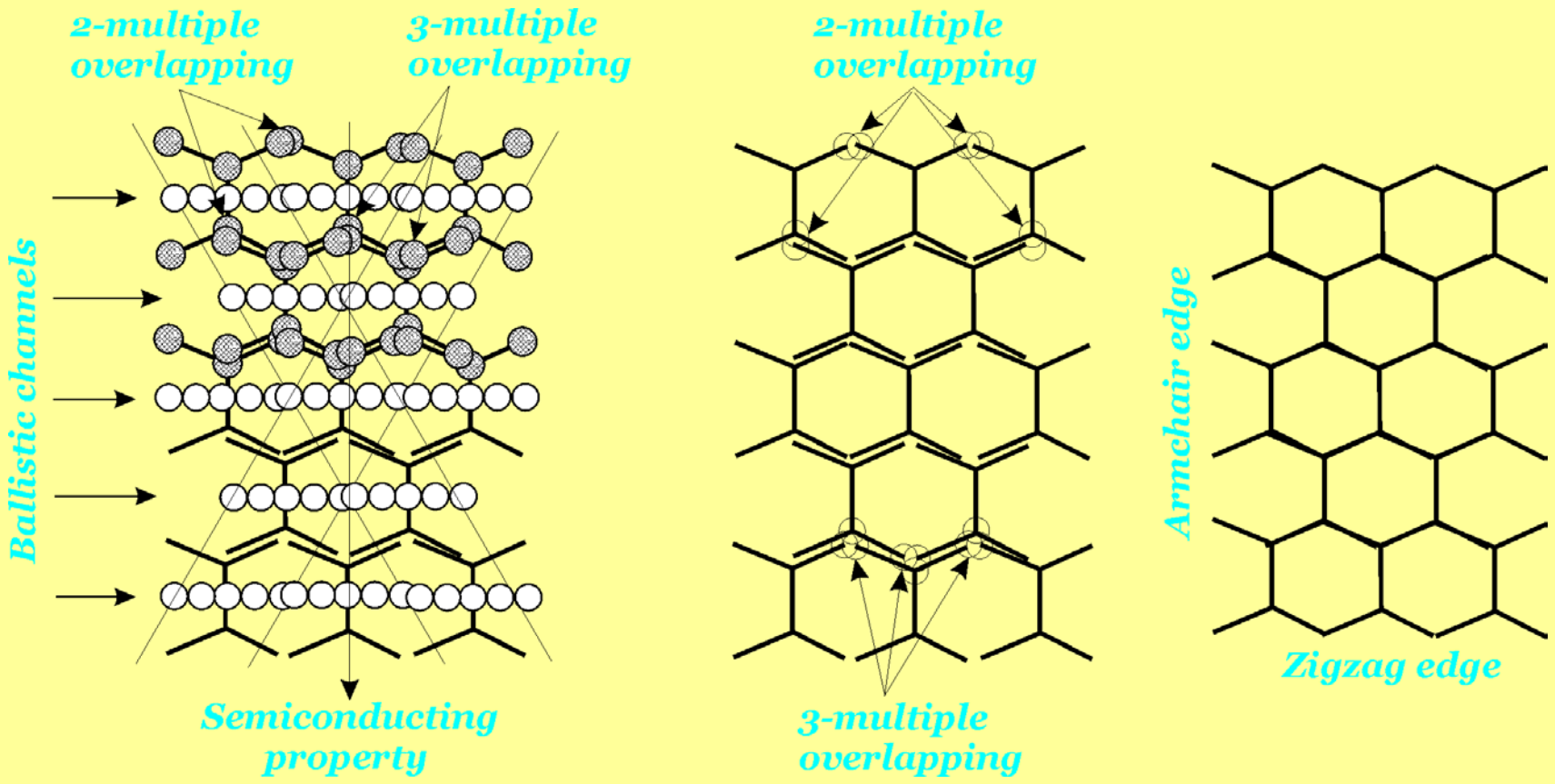

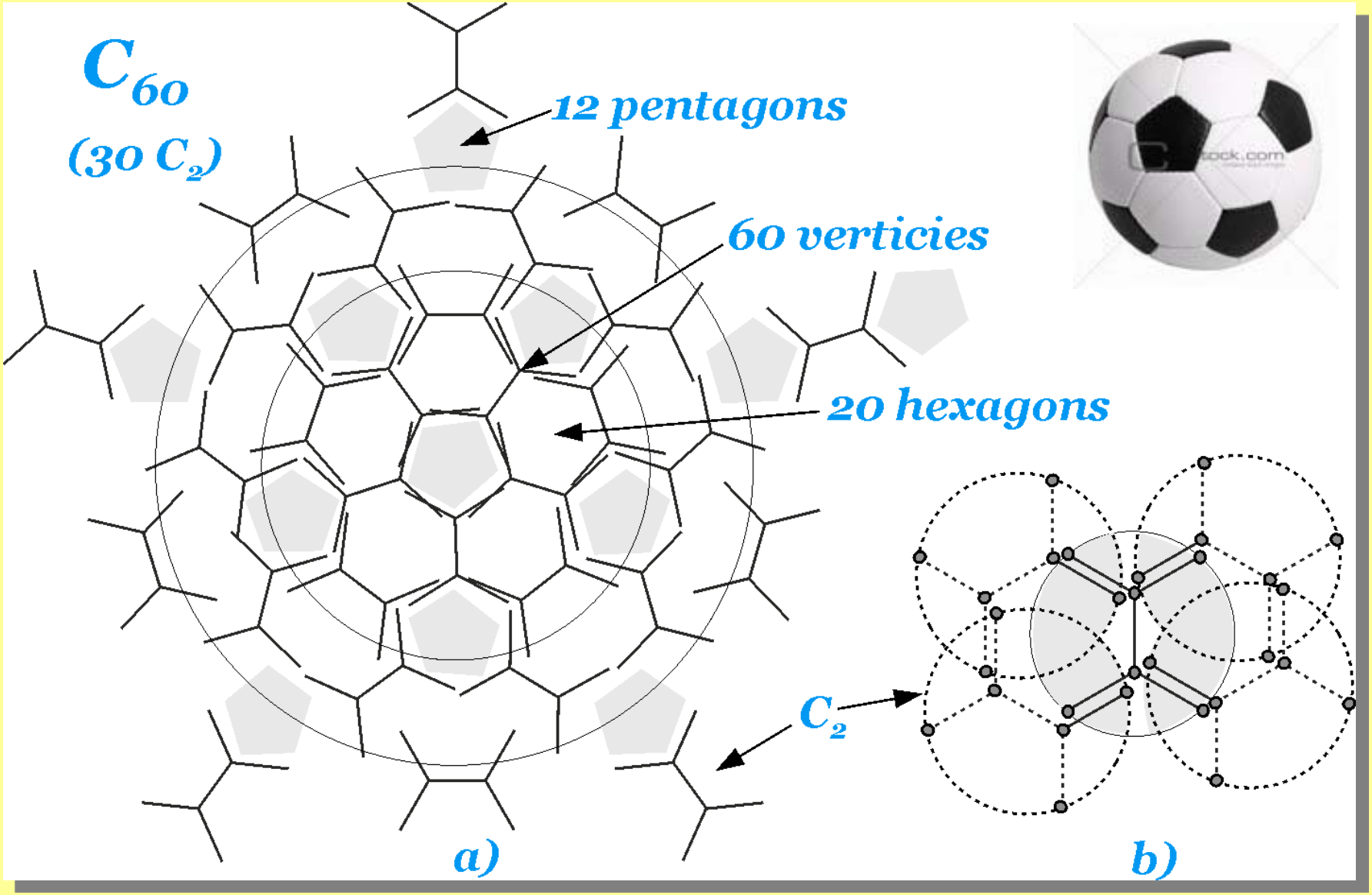

Buckminsterfullerene C_{60}

The Formation of Bonds in Diamond

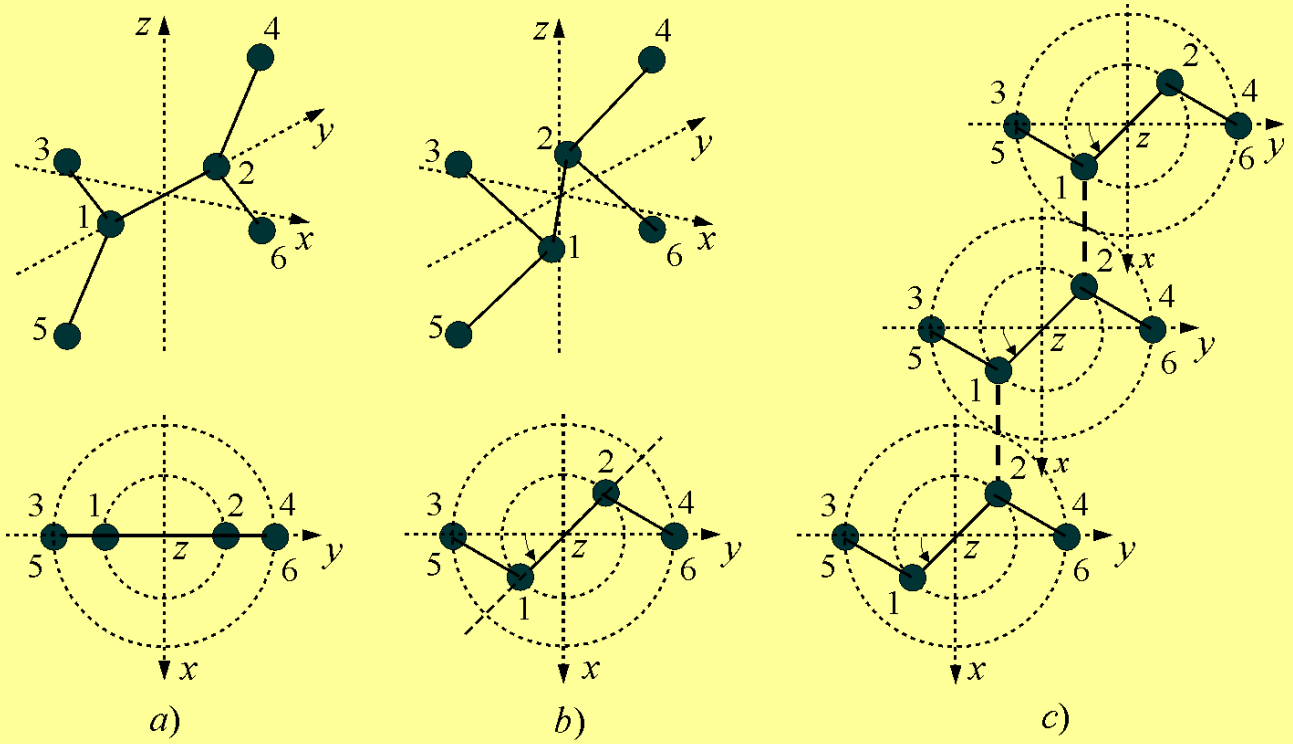

(a) A plane structure of the carbon atom (or molecule C_2);
(b) a displaced position of its internal shell with nodes 1 and 2 around the z-axis by the phase angle $\alpha = \pi/4$;
(c) the bindings (dashed lines) between displaced internal nodes 1 and 2 of different carbon dimmers, resulted in a face-centered cube structure of diamond

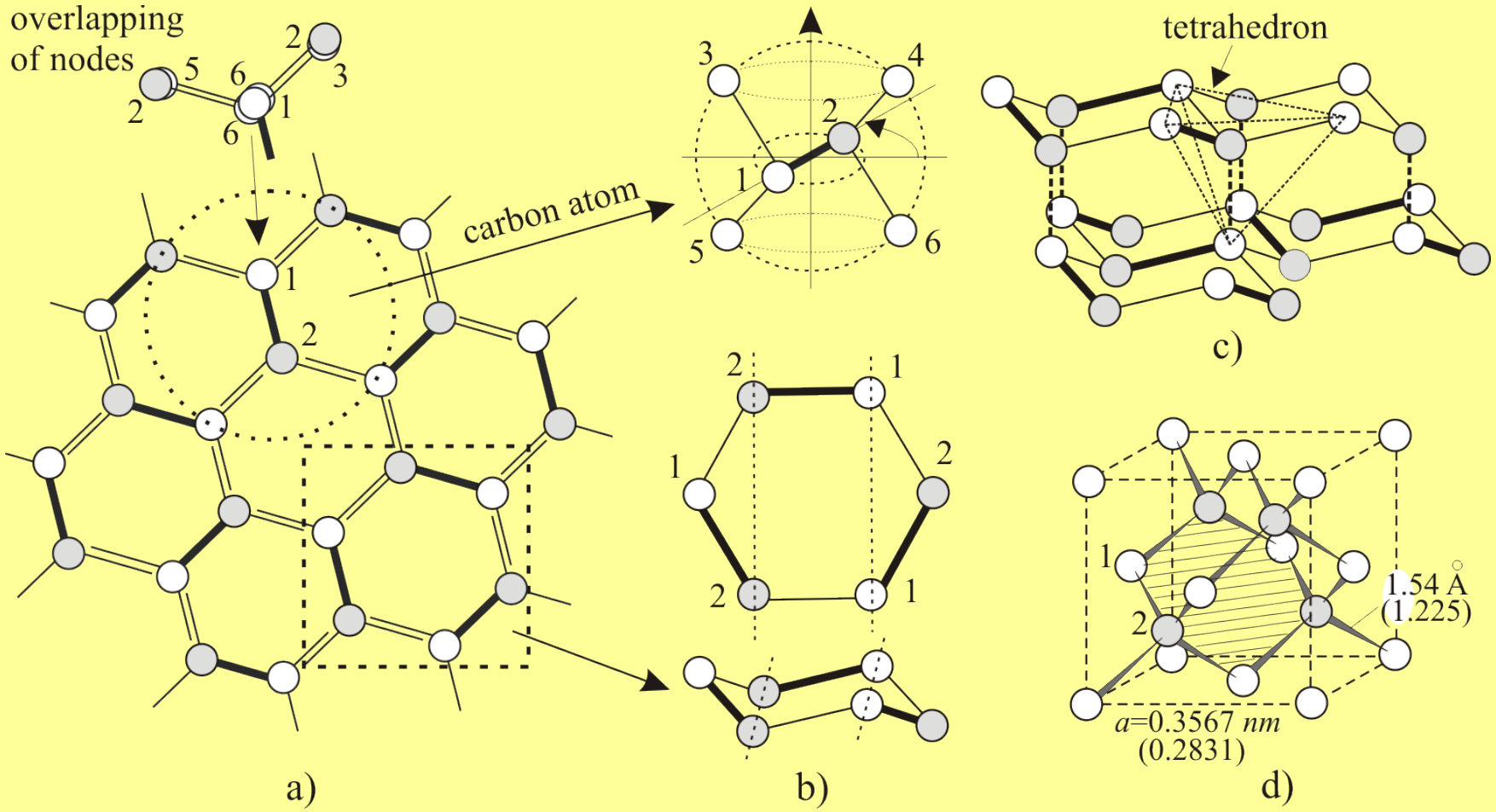

The face centered cubic diamond lattice structure

Two Possible Ways (c, d) of the Formation of the methane molecule CH_4

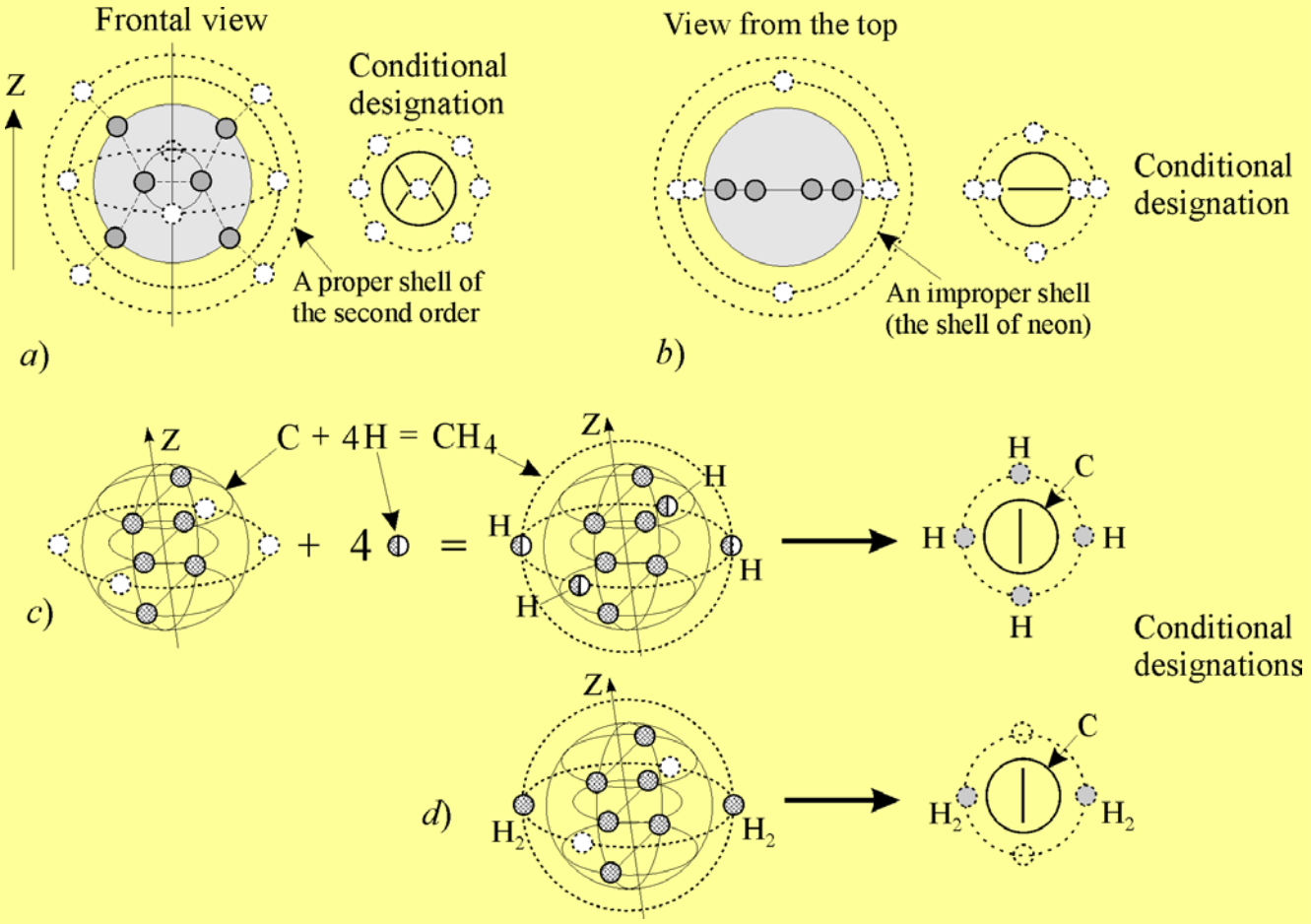

(a, b) The shell-nodal structure of carbon with indication of two nearest, proper and improper, external spherical shells with their potential polar-azimuthal nodes designated by dotted lines.

One more possible way of the formation of CH_4

(A case of the participation of the second order proper radial shell of $^{12}_{6}C$ in the formation of molecular bonds, resulted in a plane structure of the molecule)

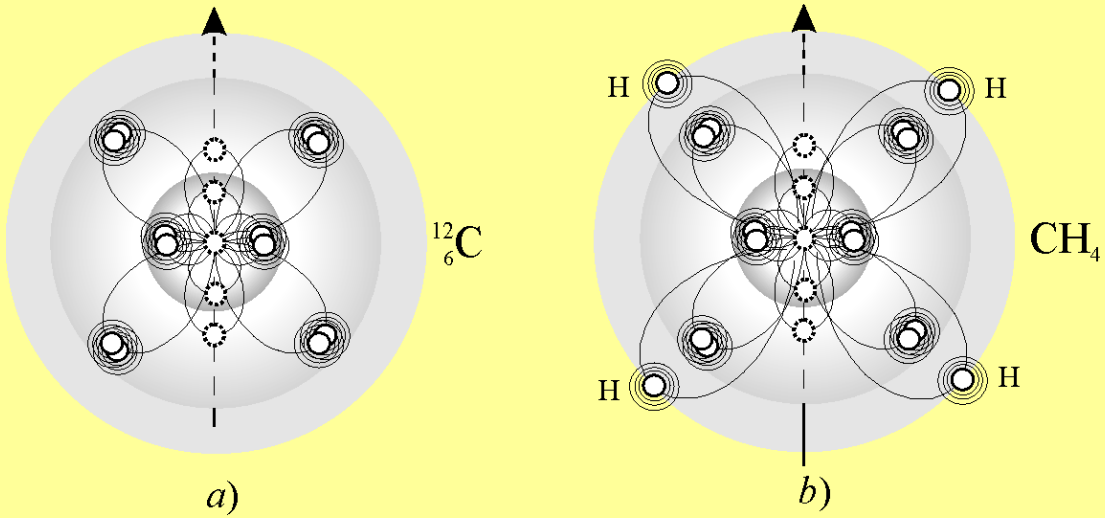

(a)An internal structure of the carbon atom $^{12}_{6}C$; (b) all chemically adsorbed individual H-atoms are in one plane with the completely filled by coupled H-atoms proper potential nodes of carbon

The Structure of Bindings in Typical Hydrocarbon Compounds

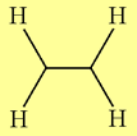

CH_4
methane

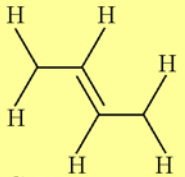

C_2H_6
ethane

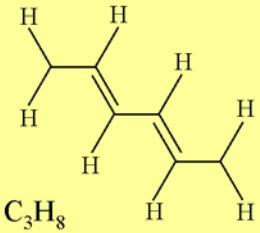

C_3H_8
propane

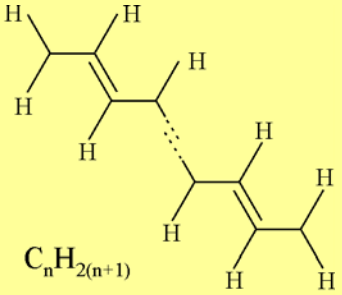

$C_nH_{2(n+1)}$

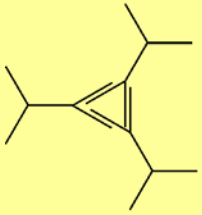

cyclopropane C_3H_6

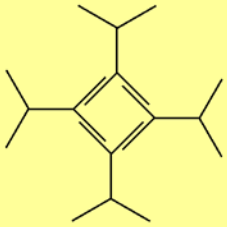

cyclobutane C_4H_8

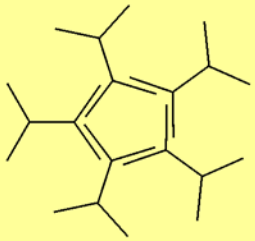

cyclopentane C_5H_{10}

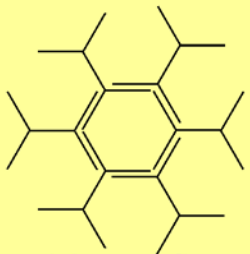

cyclohexane C_6H_{12}

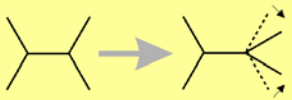

Distortion of bindings in carbon atoms of cyclopropane C_3H_6

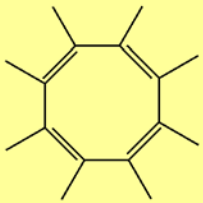

C_8H_8
cyclooctatetraene

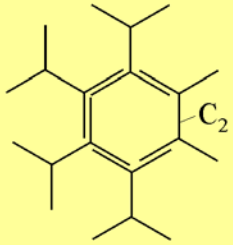

C_6H_{10}
cyclohexene

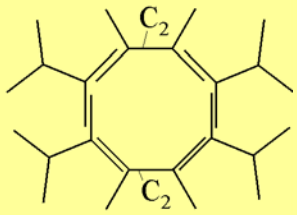

C_8H_{12}
cyclooctadiene

A schematic view showing how C – C bonds are formed in hydrocarbon compounds

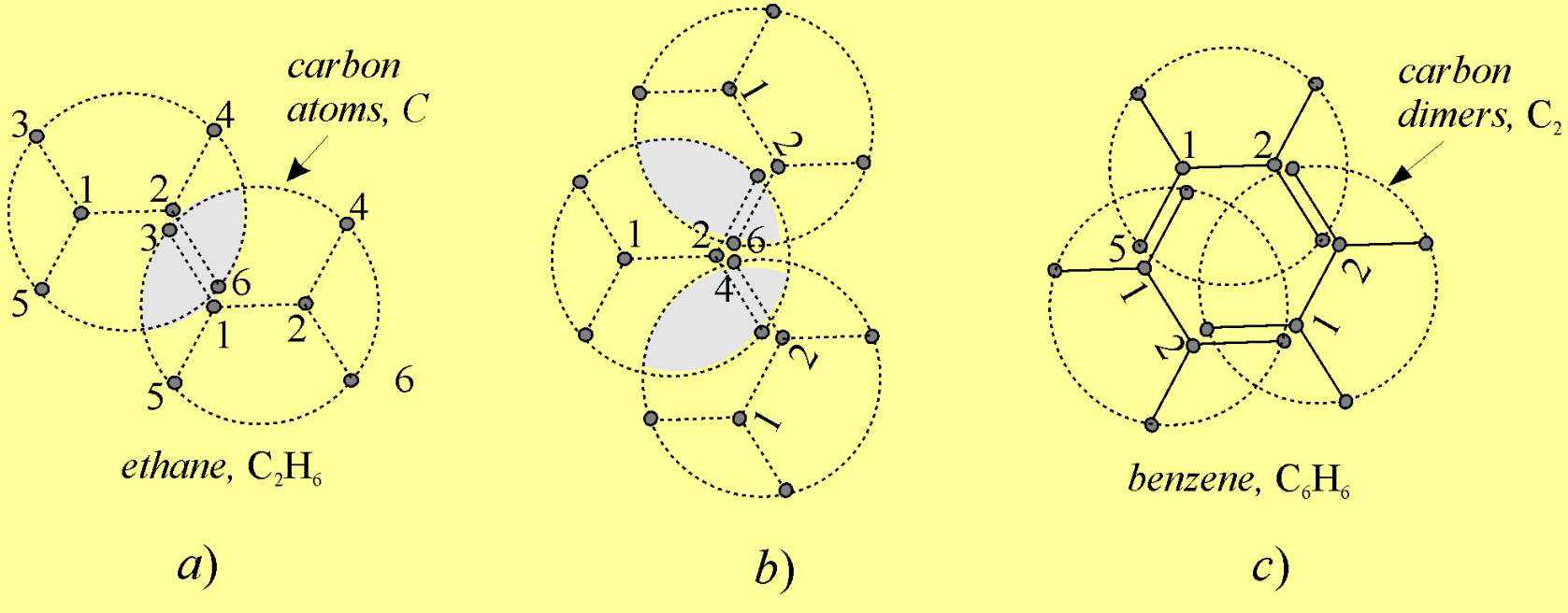

The character of overlapping (two- and three-multiple) of polar-azimuthal nodes for the case of single carbon atoms (a) and their dimmers (b, c)

Edges of graphene

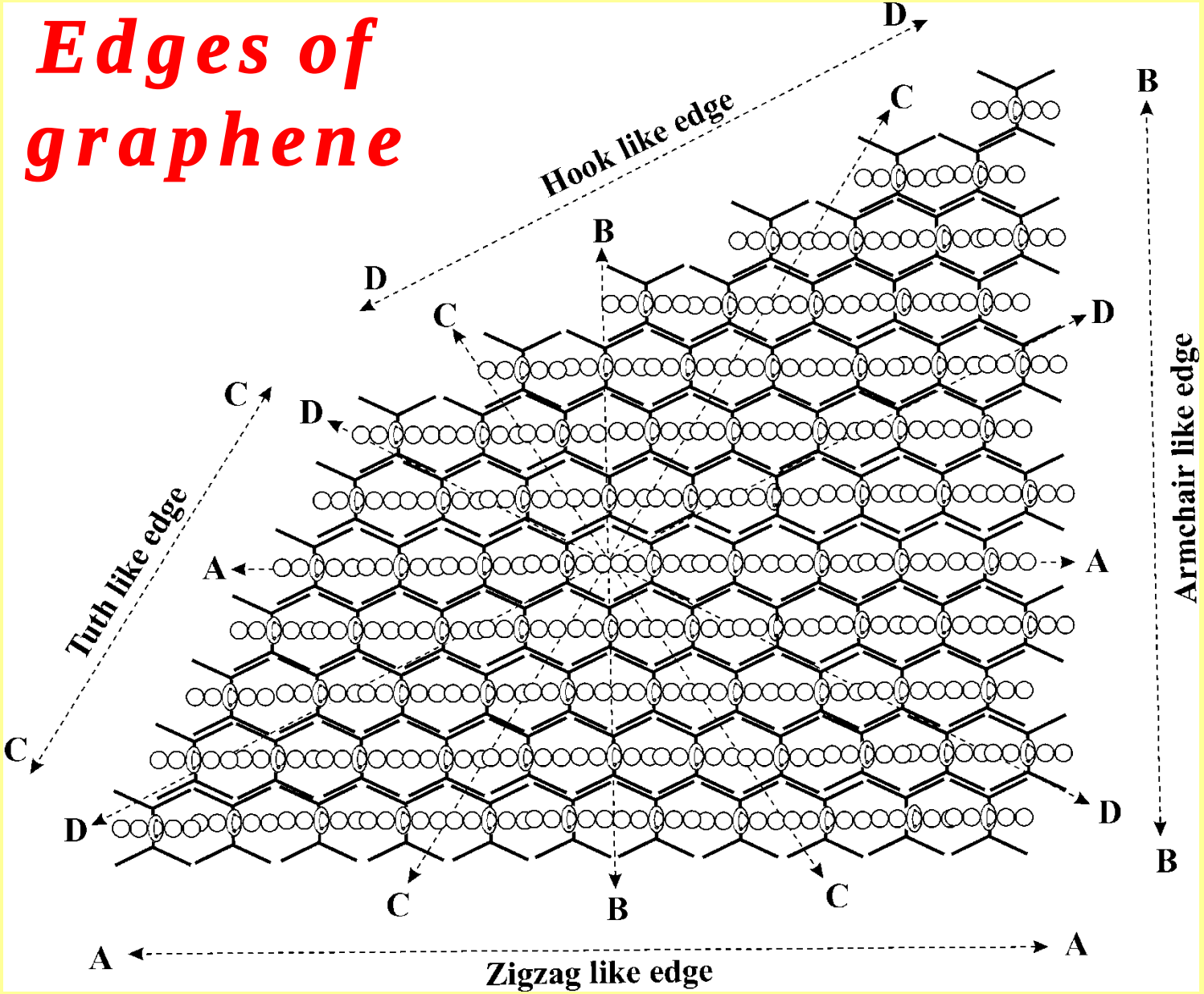

Two images of graphene edges

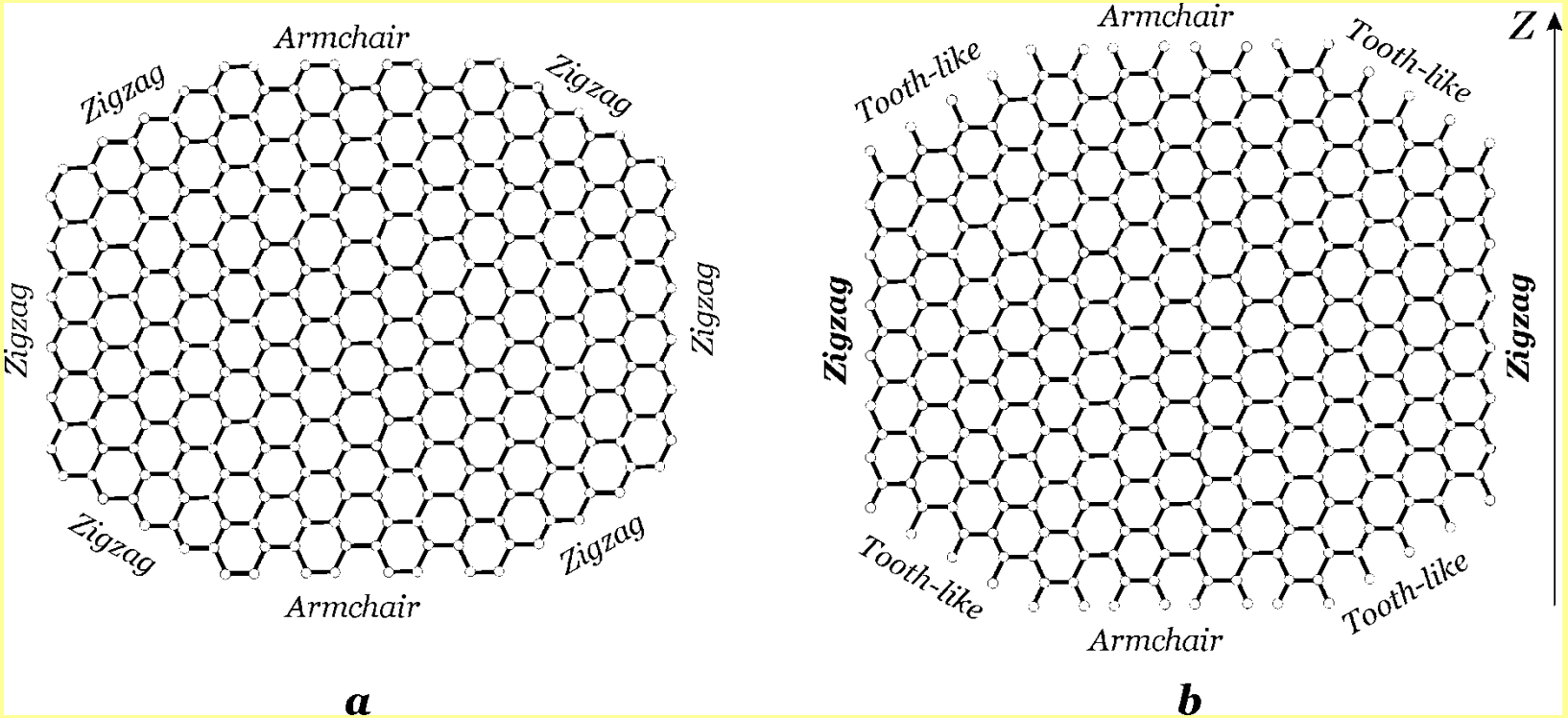

Incorrect (overall used)

Correct

Two images of graphene edges

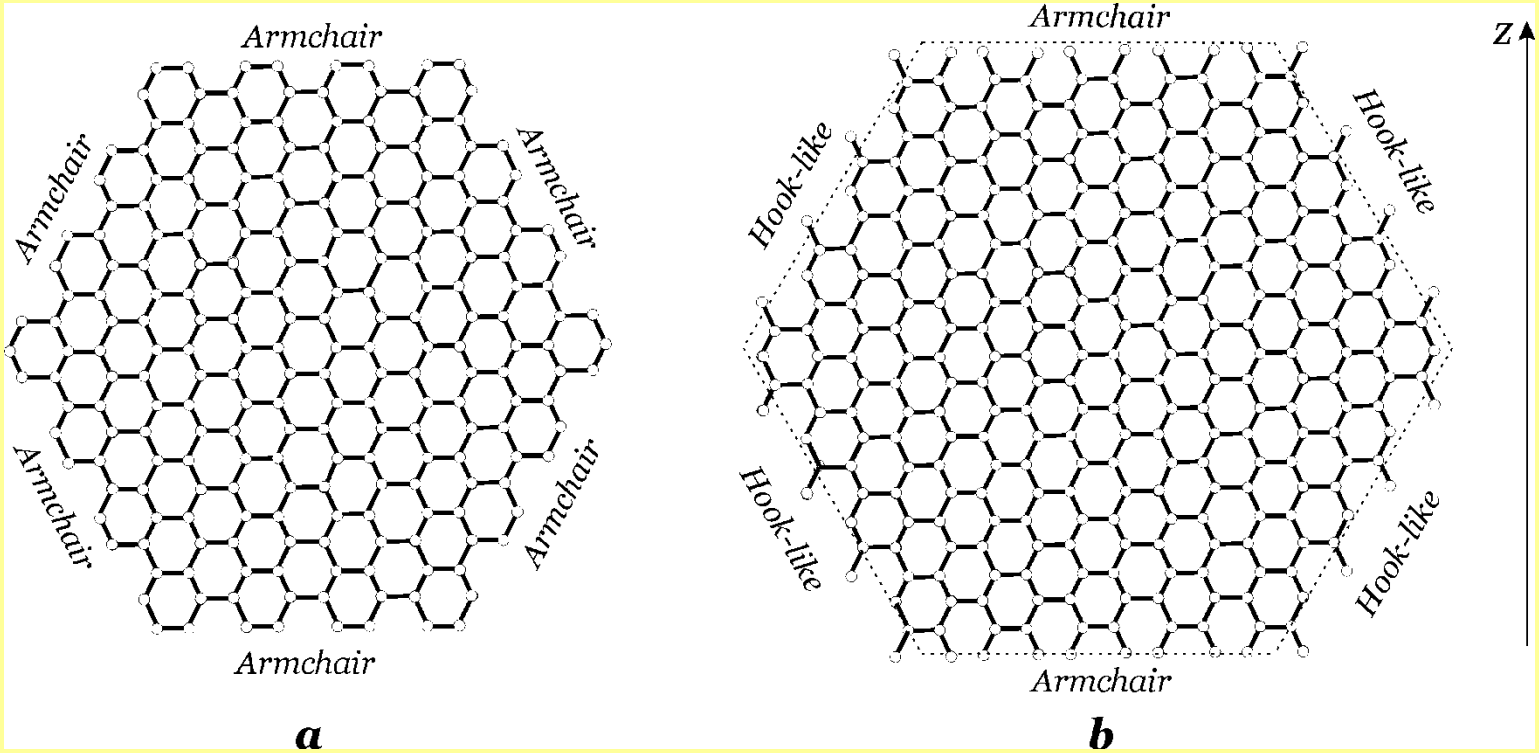

Incorrect (overall used)

Correct

Two images of graphene edges

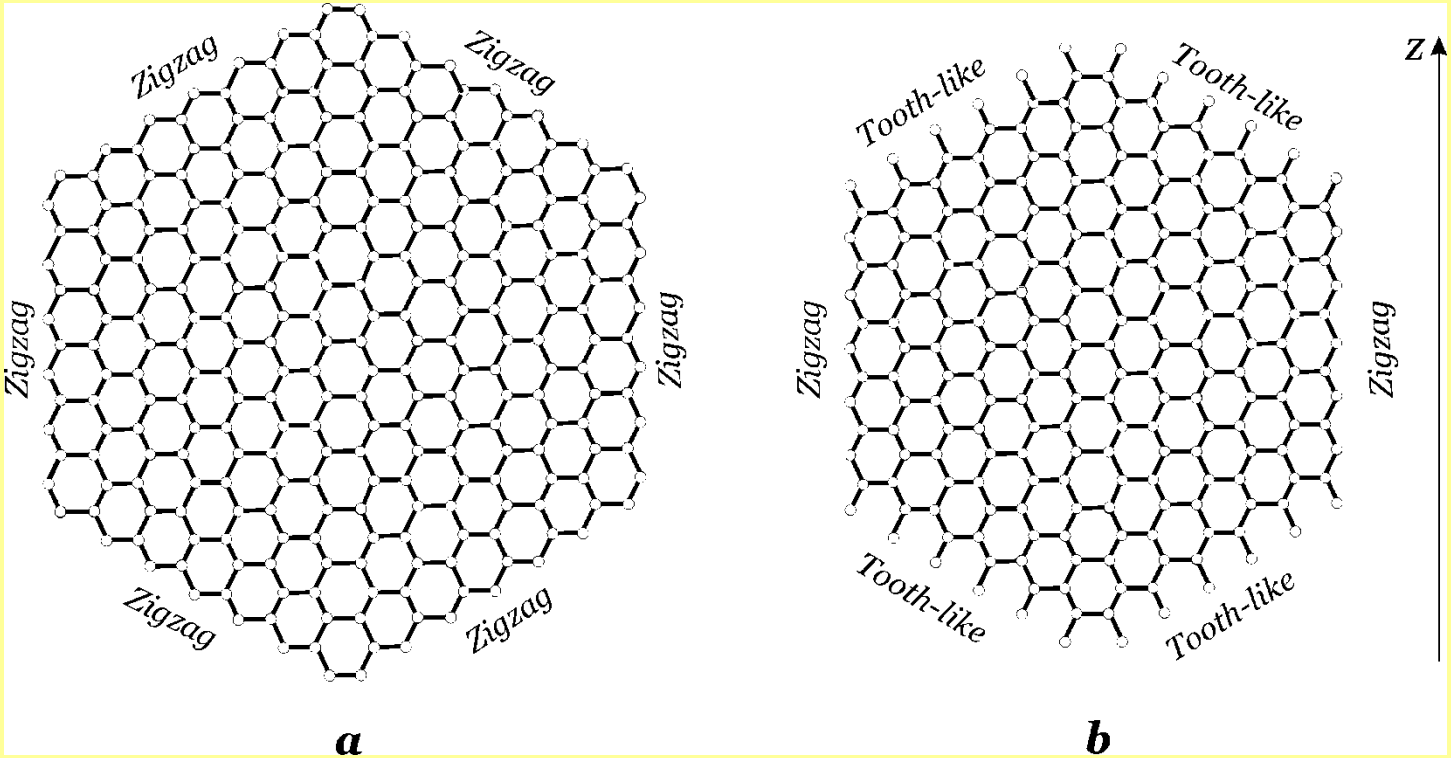

Incorrect (overall used)

Correct

*Direct Image of a Single-Layer Graphene Membrane**

(with our findings)

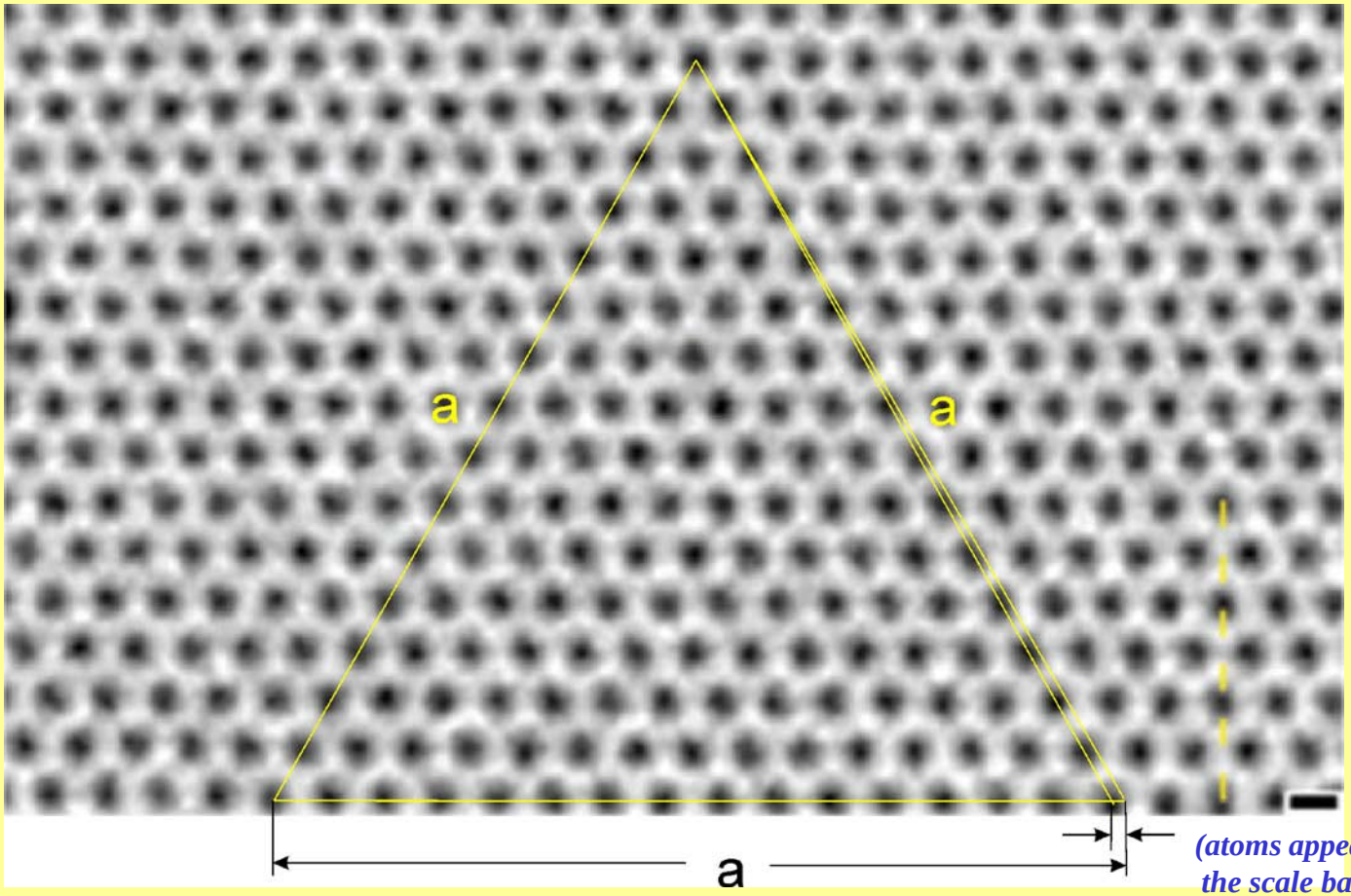

(atoms appear white, the scale bar is 2 Å)

*[J.C. Meyer, C. Kisielowski, R. Erni, M.D. Rossell, M.F. Crommie, and A. Zettl. *Direct imaging of lattice atoms and topological defects in graphene membranes*. Nano Lett. 8 (11), 3582-3586 (2008)]

Mechanism of the formation of typical metastable pentagon-heptagon (5-7) defects inherent in graphene

(two pairs of five- and seven-membered rings of carbon nodes)

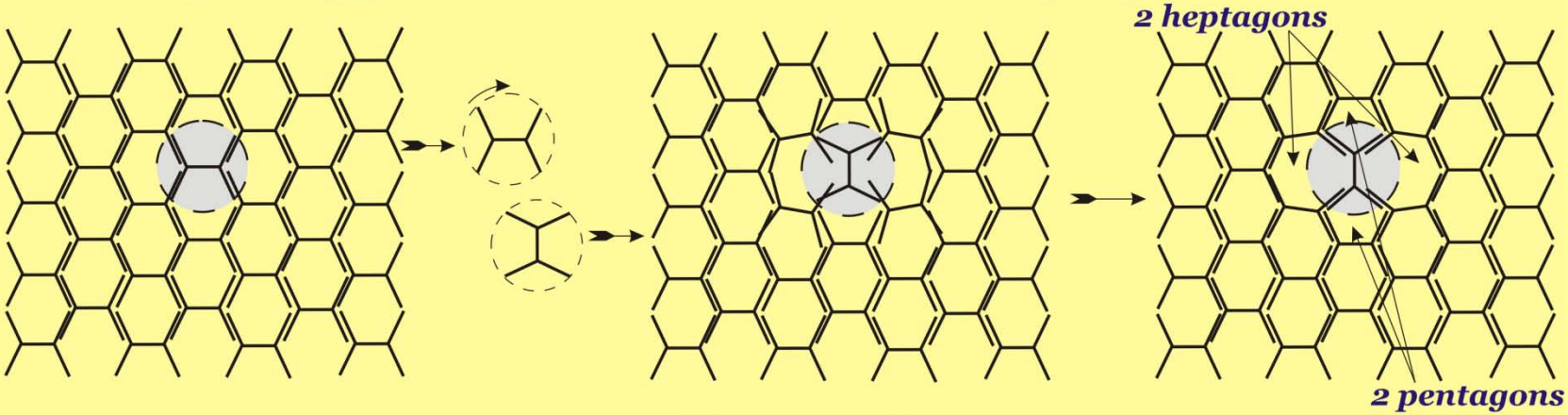

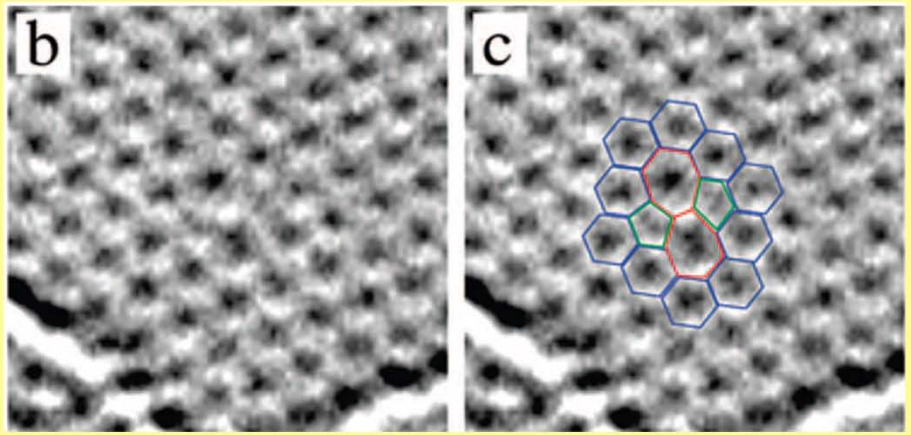

Figure 3. ...*
(b) Stone-Walles (SW) defect
(c) same image with atomic configuration superimposed

**[J. C. Meyer at al.,Direct Imaging of Lattice Atoms and Topological Defects in Graphene Membranes, Nano Lett, 2008, 8 (11), 3582-3586]*

Formation of 4 pairs of five- and seven-membered rings of carbon nodes

*"The study of defects,vacancies, and edges in graphene, as well as absorbates, is important for basic understanding of this novel material as well as for potential electronic, mechanical, and thermal applications"**

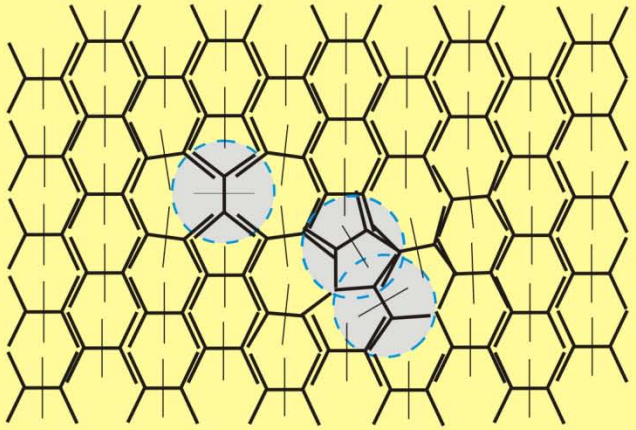

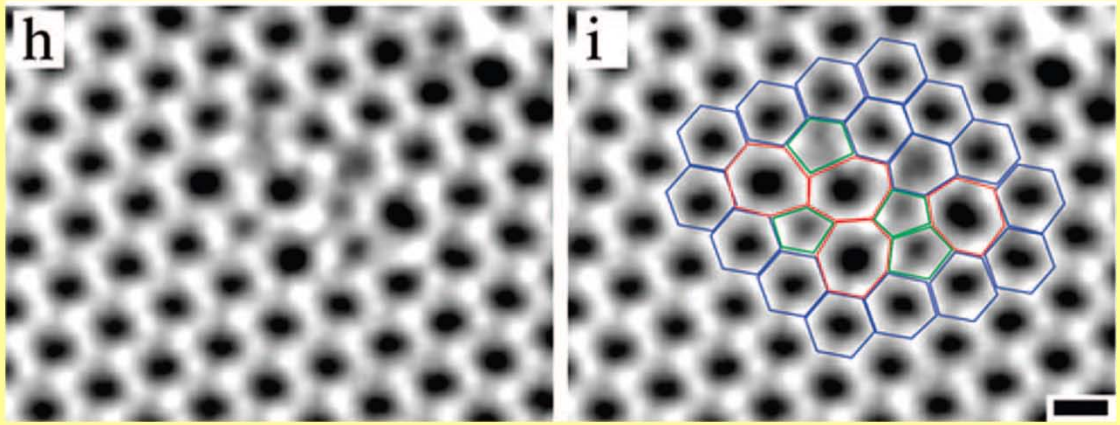

Figure 3*. ...
(h and i) Defect image and configuration consisting of four pentagons (green) and heptagons (red)

**[J. C. Meyer at al.,Direct Imaging of Lattice Atoms and Topological Defects in Graphene Membranes, Nano Lett, 2008, 8 (11), 3582-3586]*

Our comments to the article

[*Uniaxial strain in graphene by Raman spectroscopy: G peak splitting, Grüneisen parameters, and sample orientation*, Phys. Rev. B 79, 205433 (8 pages), 2009 by T. M. G. Mohiuddin at al.]

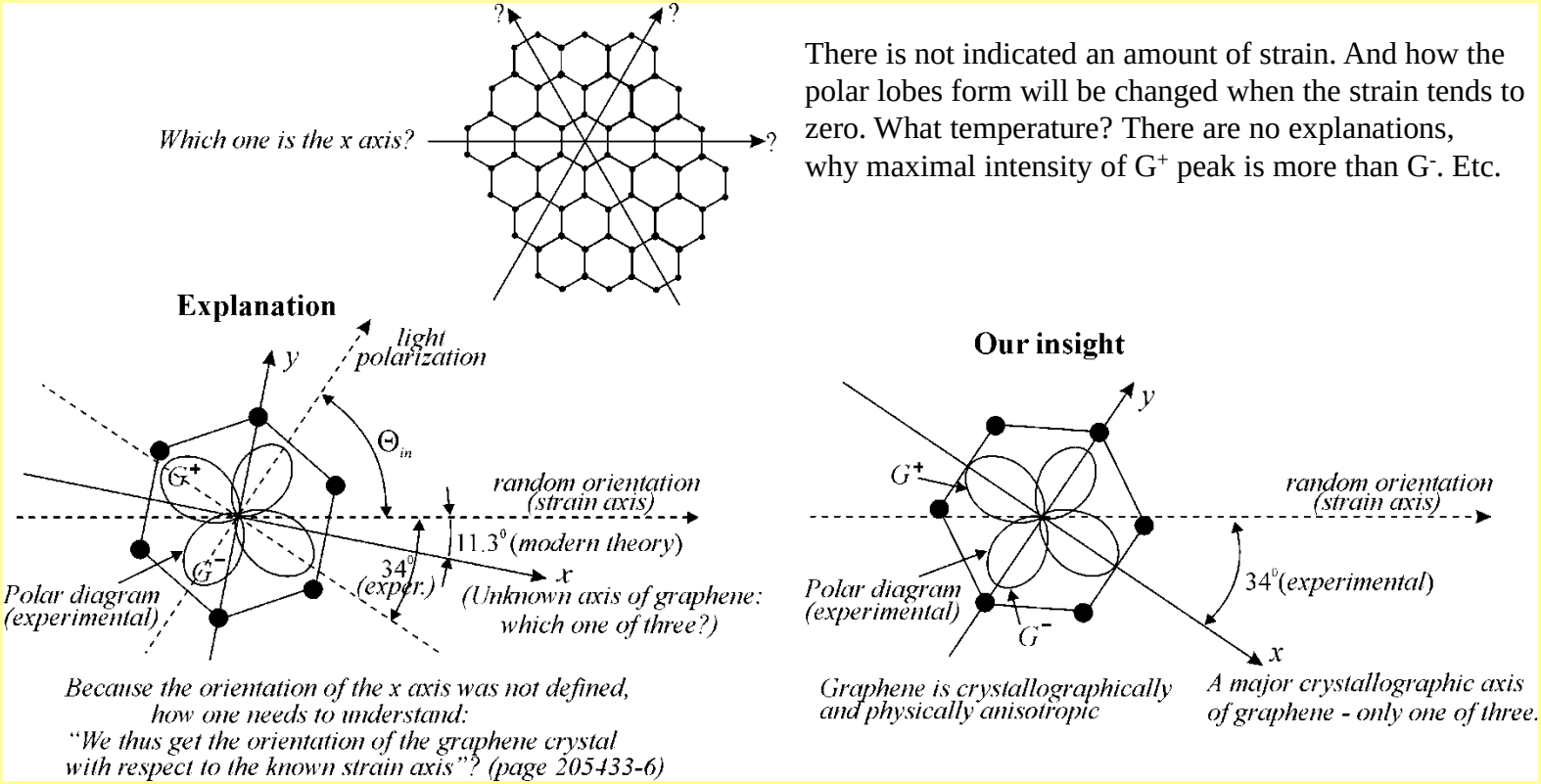

There is not indicated an amount of strain. And how the polar lobes form will be changed when the strain tends to zero. What temperature? There are no explanations, why maximal intensity of G^+ peak is more than G^-. Etc.

Mutually perpendicular axes of polar lobes are just characteristic crystallographic axes of graphene monolayer! The angles [Ref, Fig 6] between the strain axis and the axes of the lobes are equal to 34^0 and 56^0, they are accidental in value, depending on an accidentally oriented graphene monolayer on a substrate in the experiment. A small difference in a maximal intensity of G^+ and G^- peaks is related with the anisotropy of electrical conductivity. Thus, actually, authors of the paper, unknowing about this (not understanding it), have defined actually the orientation of characteristic crystallographic axes on a tested graphene monolayer, thus confirming that graphene is anisotropic.

A conditional image of the formation of the H_2O molecule, and the density of probability $\hat{\Psi}$ (contour plots) of the localization of matter in an external shell for the planes x = 0, y = 0, and z = 0

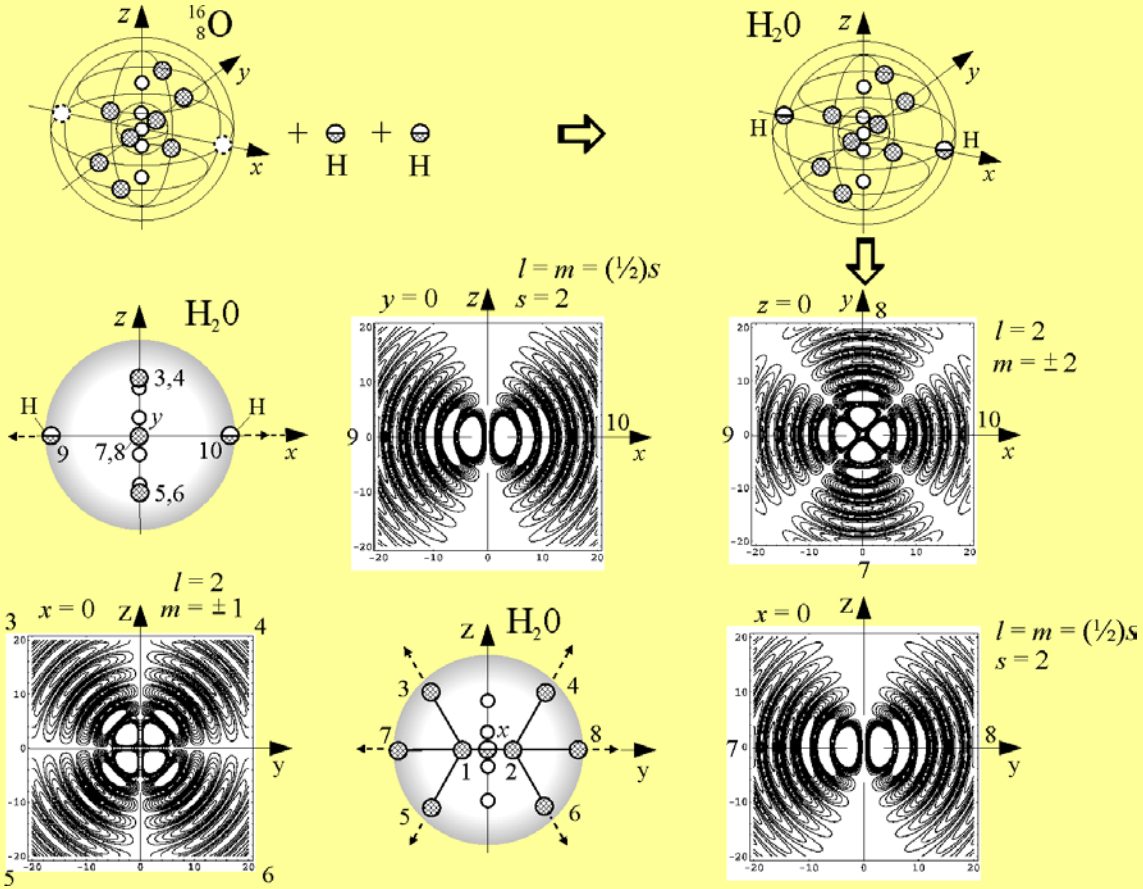

The dashed smaller arrows in the pictures indicate the main directions of external internodal bindings inherent in the water molecule

A Possible Way of the Formation of the oxygen molecule O_2

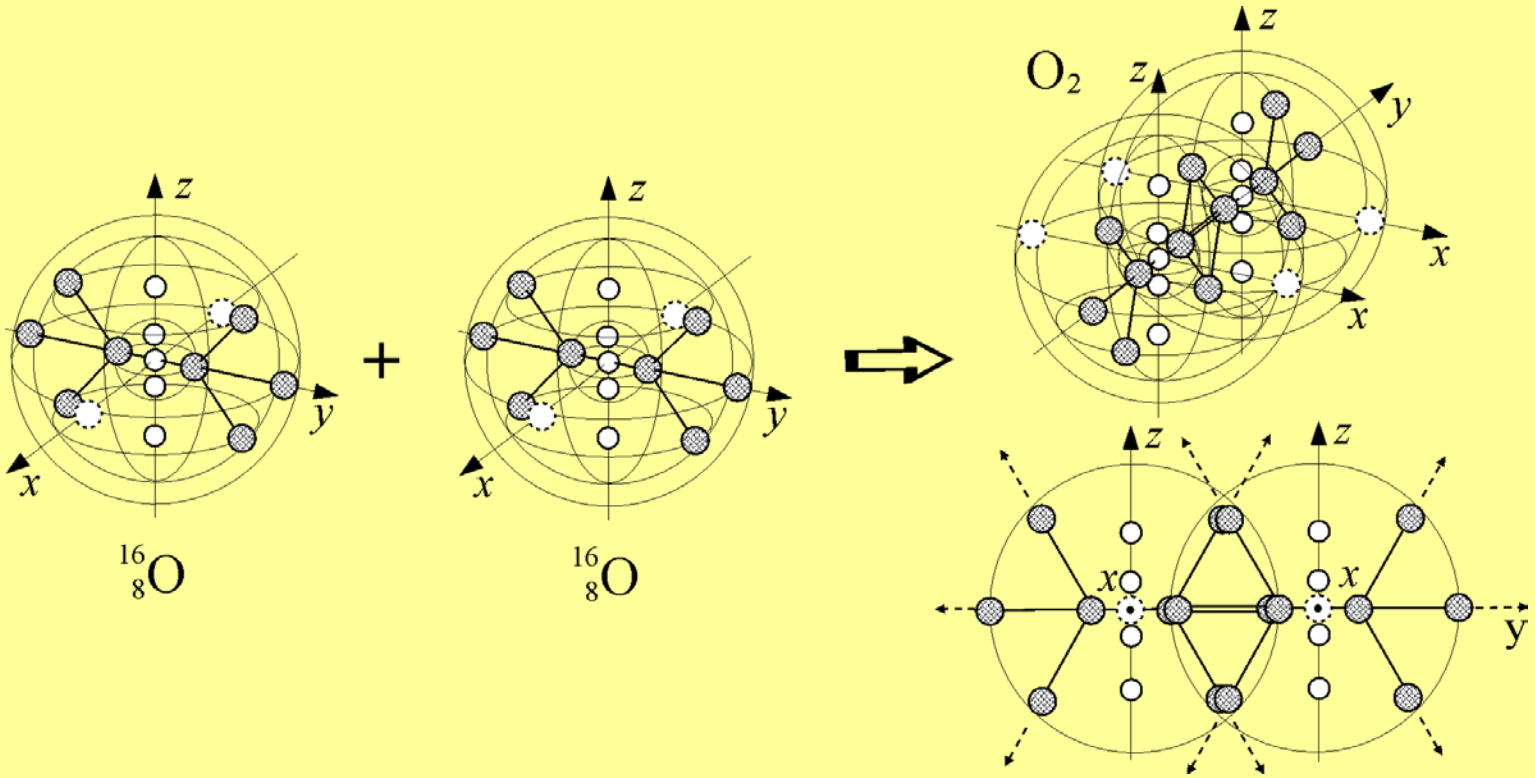

One More Possible Way of the O_2 Formation

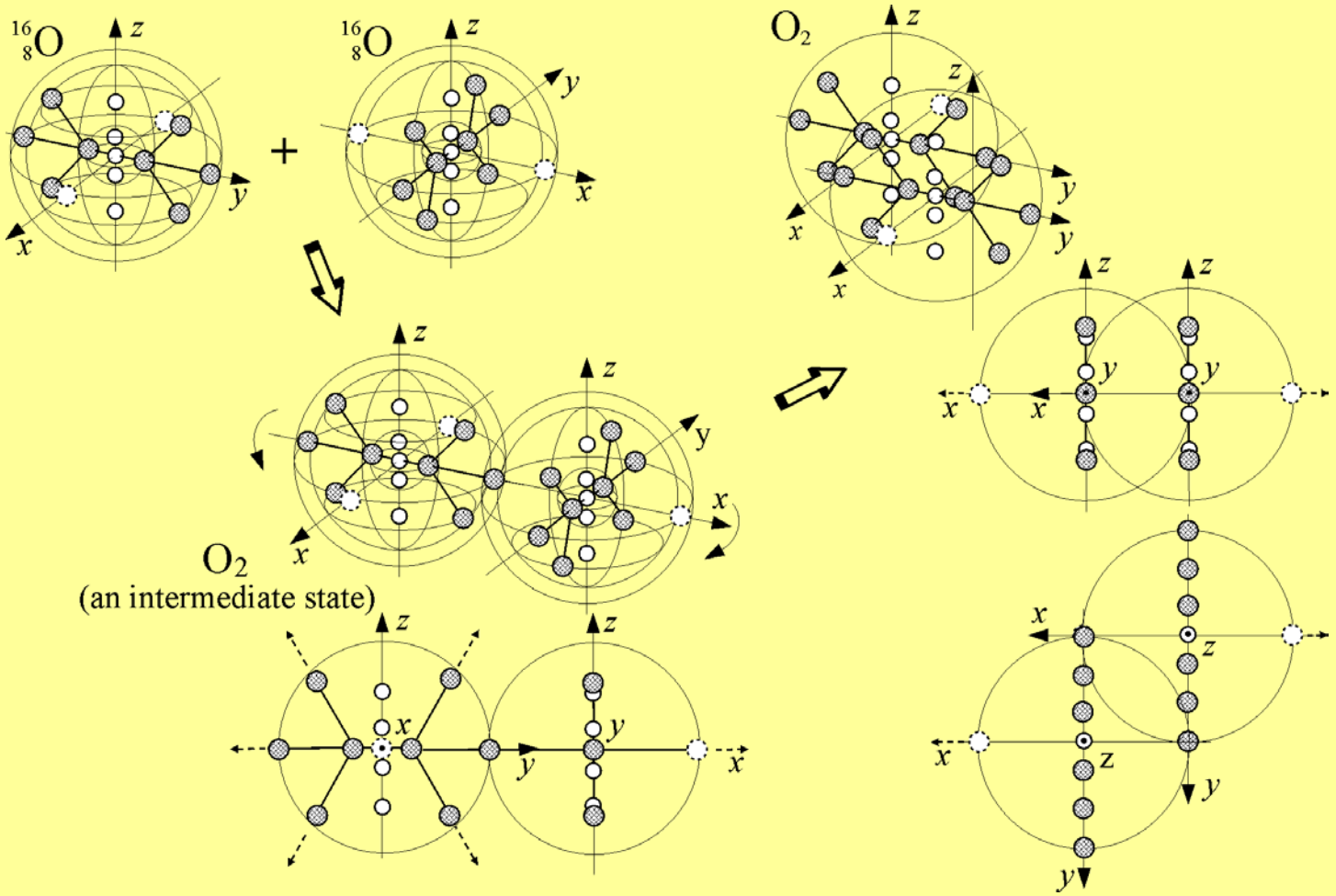

One more possible way of the formation of oxygen O_2, and the possible nodal structure of carbon oxide CO, carbon dioxide CO_2, and the ozone molecule O_3 (a)

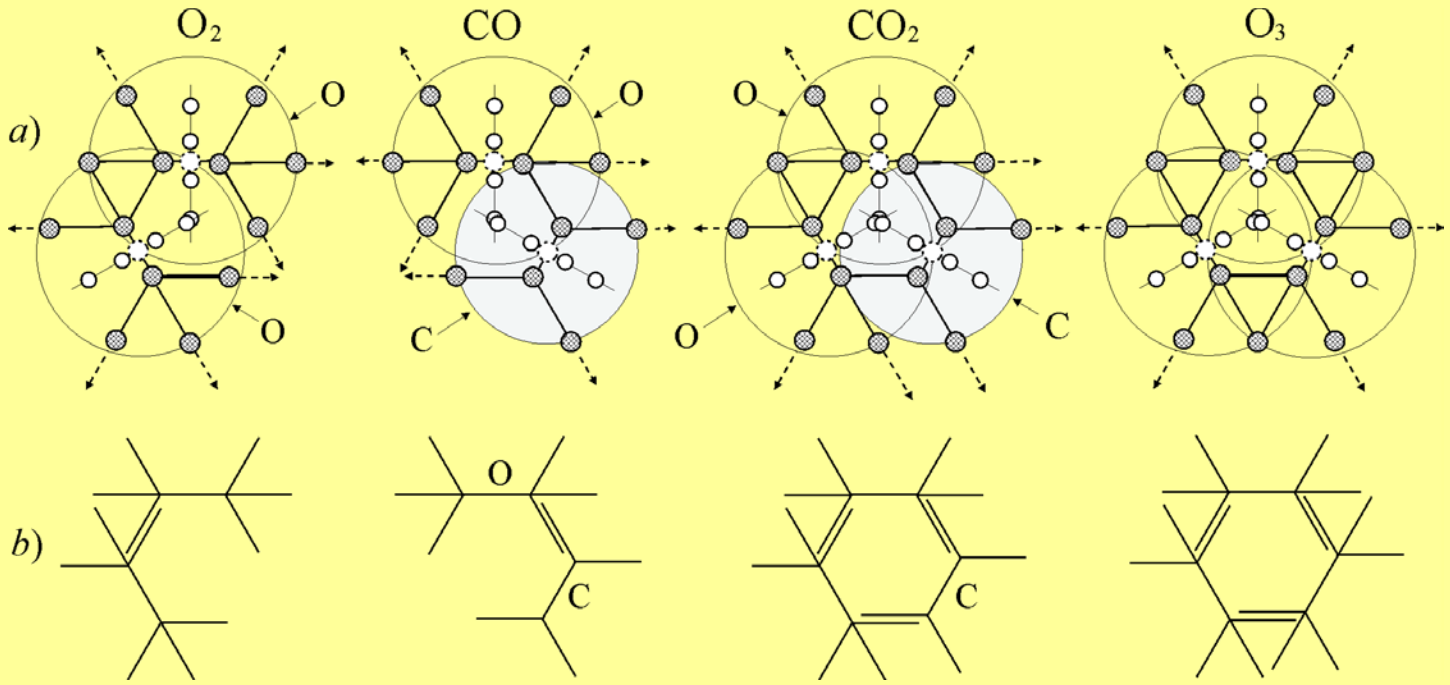

(b) symbolic designations of the compounds distinguished by the two-multiple overlapping of proper nodes of constituent atoms

Two possible ways of the formation of hemioxide N_2O

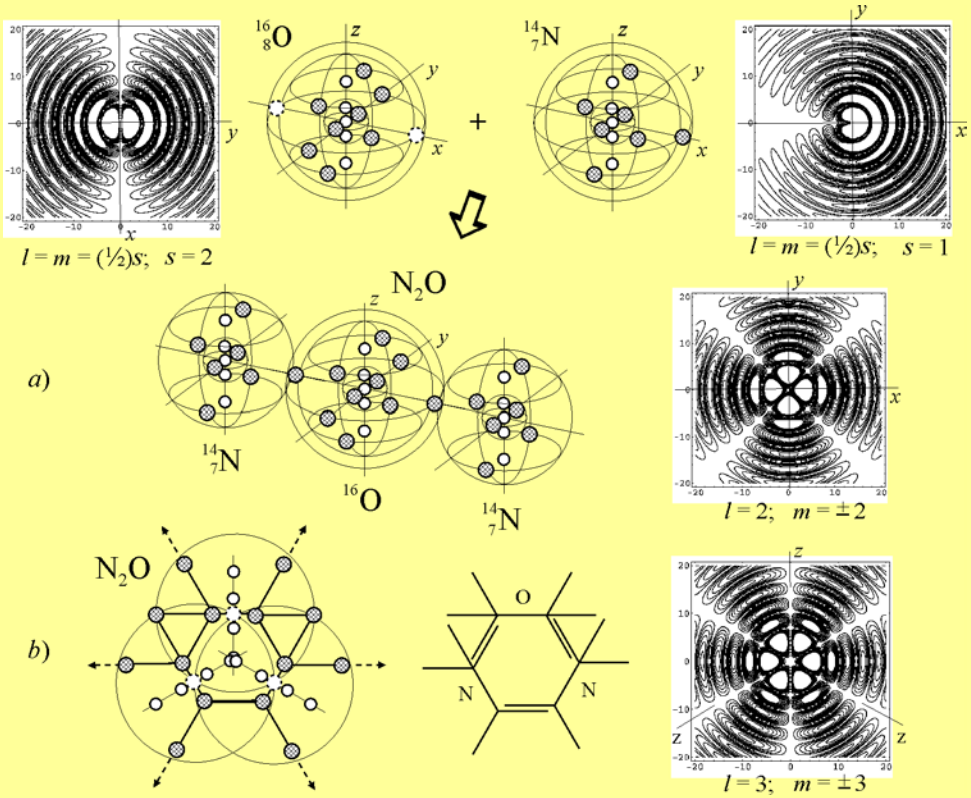

(a) an intermediate (unfolded) image of one of the ways, (b) another of the possible nodal bindings in the hypothetical N_2O structure. The equatorial densities of probability $\hat{\Psi}$ (contour plots) are drawn for external shells of separate atoms, $^{16}_{8}O$ and $^{14}_{7}N$ (the upper row, left and right); for the shell at l = 2, $m = \pm 2$ (the section for z = 0); and for the external shell of the resulting formation (l = 3, $m = \pm 3$)

The Shell-Nodal Structure of the Aluminum Oxide Al2O3

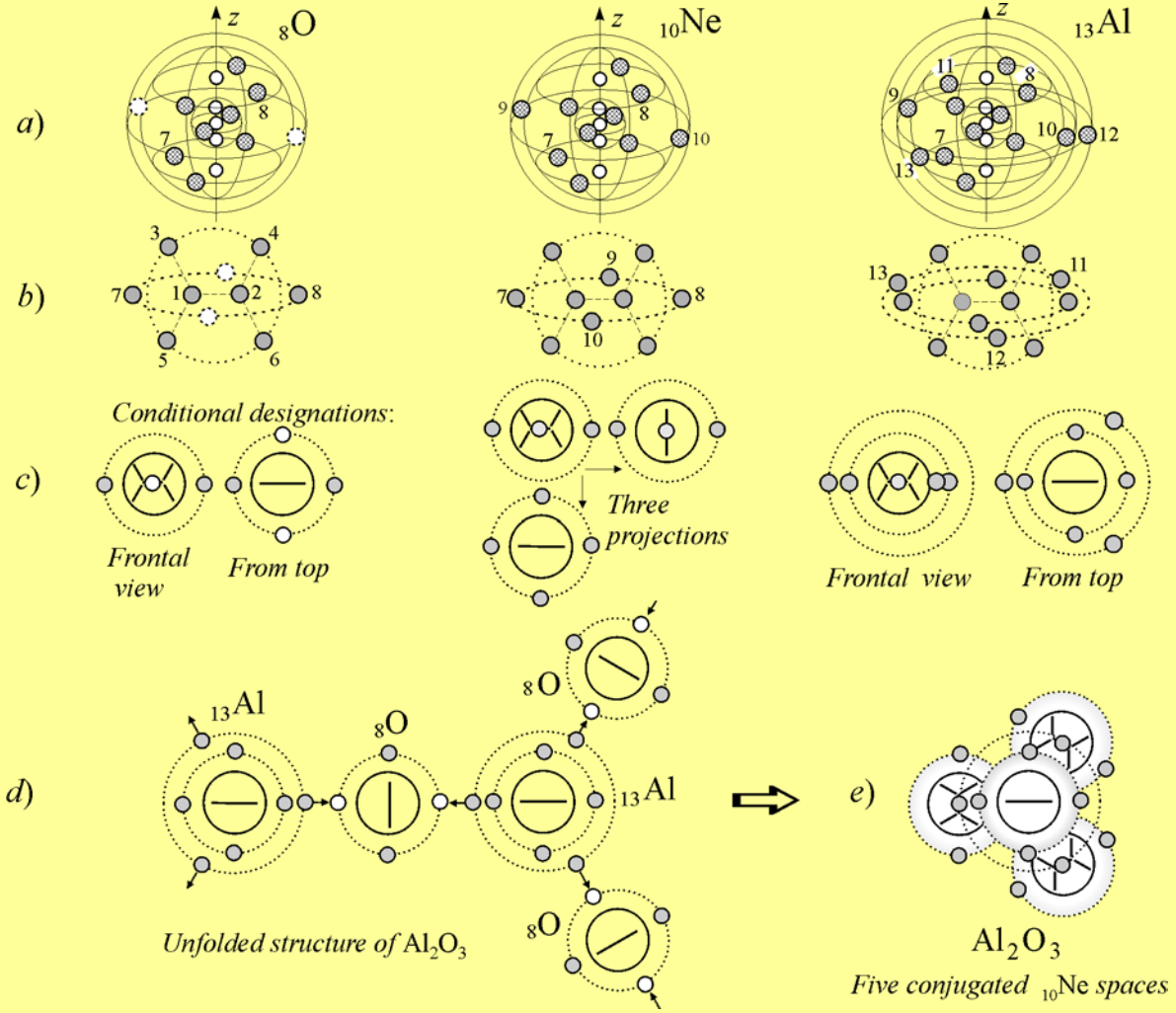

(a, b, c) the nodal structure of the atoms O, Ne, and Al and their conditional designations for different projections; the unfolded (d) and closed (e) conditional images of the resulting Al_2O_3 structure

Formation of One-Atom-Thick Layer of Hexagonal Boron Nitride

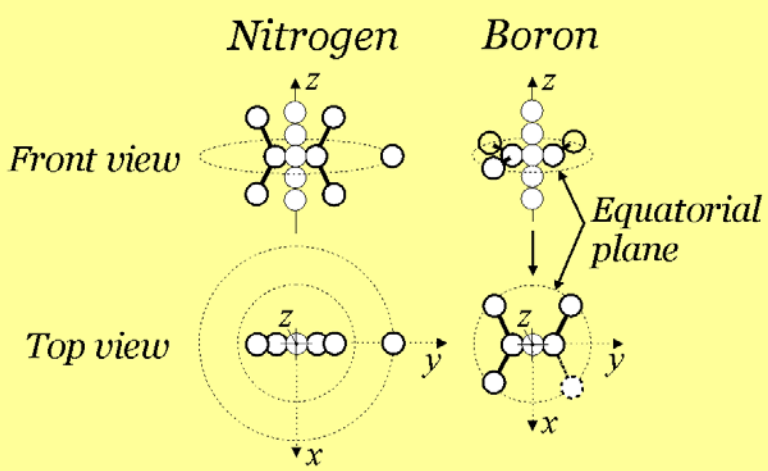

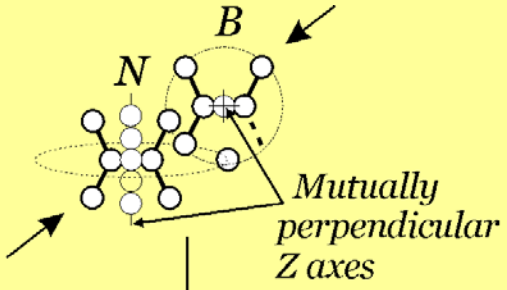

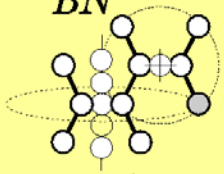

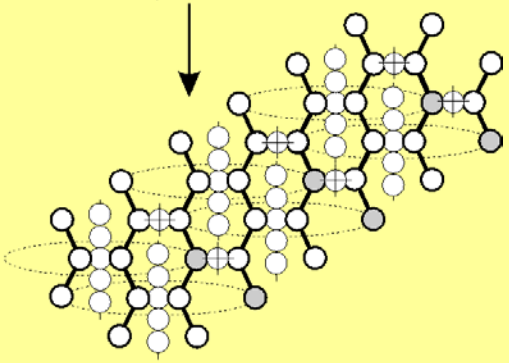

The structure of hexagonal BN

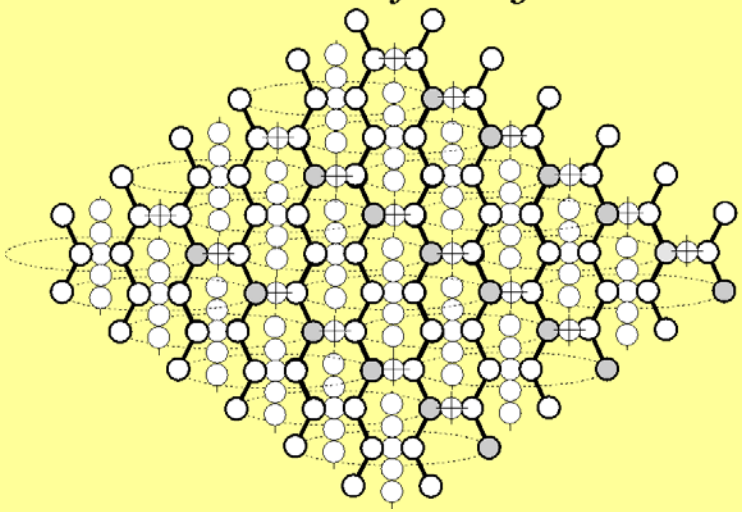

CONCLUSION

We are on a threshold of uncovering the “genetic code” of structural variety in nature

http://shpenkov.janmax.com/CarbonOxygen.pdf